Dissertation

Glycine – antitumorigenic and cardioprotective substance in a model of colorectal cancer liver metastasis treatment by FOLFOX chemotherapy

submitted by

Mag. Juste Bausiene

for the Academic Degree of

Doctor of Medical Science

at the

Medical University of Graz

Department of Surgery, General, Visceral and Transplant Surgery

under the Supervision of

Assoz. Prof. Priv.-Doz. Dr.med.univ. Philipp Stiegler

2023

Statutory Declaration

I hereby declare that this thesis is my own original work and that I have fully acknowledged by name all of those individuals and organisations that have contributed to the research for this thesis. Due acknowledgment has been made in the text to all other material used. Throughout this thesis and in all related publications I followed the “Guidelines of the Medical University of Graz on Good Scientific Practice“.

Juste Maneikyte,

Date 2023-01-20

Disclosure

Part of this thesis has been published previously:

1. *Maneikyte J, Bausys A, Leber B, Feldbacher N, Hoefler G, Kolb-Lenz D, Strupas K, Stiegler P, Schemmer P. Dietary Glycine Prevents FOLFOX Chemotherapy-Induced Heart Injury: A Colorectal Cancer Liver Metastasis Treatment Model in Rats. Nutrients. 2020 Aug 28;12(9):2634. doi: 10.3390/nu12092634. PMID: 32872376; PMCID: PMC7551625.*
2. *Maneikyte J, Bausys A, Leber B, Horvath A, Feldbacher N, Hoefler G, Strupas K, Stiegler P, Schemmer P. Dietary glycine decreases both tumor volume and vascularization in a combined colorectal liver metastasis and chemotherapy model. Int J Biol Sci. 2019 Jun 4;15(8):1582-1590. doi: 10.7150/ijbs.35513. PMID: 31360101; PMCID: PMC6643216.*

All co-authors listed below actively contributed to the results of the thesis and the publications resulting from the thesis project:

Augustinas Bausys[1], Bettina Leber[1], Angela Horvath[2], Nicole Feldbacher[1], Gerald Hoefler[3], Dagmar Kolb-Lenz[4], Kestutis Strupas[5], Peter Schemmer[1], Philipp Stiegler[1].

1-General, Visceral and Transplant Surgery, Department of Surgery, Medical University of Graz, 8036 Graz, Austria.
2-Gastroenterology and Hepatology, Dept. of Internal Medicine, Medical University of Graz, Austria.
3-Diagnostic and Research Institute of Pathology, Medical University of Graz, 8010 Graz, Austria.
4-Institute of Cell Biology, Histology, and Embryology, Medical University Graz, 8010 Graz, Austria.
5-Faculty of Medicine, Vilnius University, 03101 Vilnius, Lithuania.

I confirm that all co-authors have explicitly agreed and given written consent to the use of their data in this thesis.

Some parts of the thesis have been quoted verbatim from the previously published, theses project-related, articles listed above. The permission to reproduce text, figures, tables, and other content published in *International Journal of Biological Sciences* and *Nutrients* from the respective copyright holders IVYSPRING and MDPI.

Acknowledgments

Doctoral student Juste Maneikyte received funding for consumable costs and publication fees from the Medical University of Graz through the Doctoral School Molecular Medicine and Inflammation.

Contents

Abbreviations and Definitions

5-FU: 5-fluorouracil

BNP: brain natriuretic peptide

CAB: chromotrope aniline blue

CBC: complete blood count

CC531: rat colorectal cancer cell line

CCD: charge-coupled device

CRC: colorectal cancer

CRLM: colorectal liver metastasis

CTx: chemotherapy

ELISA: enzyme-linked immunosorbent assay

FABL: α-fluoro-β-alanine hydrochloride

FAC: fluoroacetate

FHPA: a-fluoro-f-hydroxypropionic acid

FOLFOX: chemotherapy scheme of 5-fluorouracil, oxaliplatin, and leucovorin;

HCM: human cardiac myocyte

h-FABP: heart fatty acid-binding protein

HGB: hemoglobin

IC50: half maximal inhibitory concentration

LV: left ventricle

LVEDD: left ventricular end-diastolic diameter

LVEF: left ventricle ejection fraction

LVESD: left ventricular end-systolic diameter

MTT: 3-(4,5-dimethylthiazol-2-yl)5-diphenyltetrazolium bromide

MVD: tumor microvascular density

OX: oxaliplatin

PBS: phosphate-buffered saline

RBC: red blood cell

VEGF: vascular endothelial growth factor

WBC: white blood cell

Abstract in German

Das Kolorektalkarzinom ist eine der häufigsten Krebsarten weltweit mit einer Inzidenz von 1 Million Betroffenen jährlich. Fast jeder zweite Patient mit dieser Diagnose entwickelt im Laufe der Zeit Metastasten in anderen Organen. Die Leber ist hierbei das am häufigsten betroffene Organ. Systemische Chemotherapie, wie zB FOLFOX, wird vor der chirurgischen Resektion angewendet, um das Langzeitüberleben von Patienten zu verbessern oder die Resektion überhaupt erst zu ermöglichen. Allerdings können Chemoresistenz und Chemotoxizität die Behandlungseffizienz empfindlich beeinträchtigen. Nebenwirkungen wie die selten auftretende, aber potenziell letale und bis dato unvermeidbare Kardiotoxizität müssen bestmöglich vermieden werden.

Glycin war in vielen Krebsarten bereits erfolgreich in der Hemmung des Tumorwachstums. Außerdem reduziert es die Thrombozyten Aggregation, verbessert die Mikroperfusion und weist sowohl hepatoprotektive, als auch antioxidative Eigenschaften auf. Daher wurde diese Studie konzipiert, um zu untersuchen, ob Glycin, in Kombination mit konventioneller FOLFOX Chemotherapie, im Setting des Kolorektalkazinoms onkologisch wirksam ist. Weiters werden eventuelle kardioprotektive Eigenschaften gegen die Chemotherapie Induzierte Kardiotoxizität untersucht. Der Effekt von Glycin wurde in vitro mit Hilfe der Kolorektalkarzinom Zelllinie (CC531) und humanen Kardiomyozyten (HCM) untersucht. In vivo wurden die Effekte von Glycin in einem Wag/Rij Rattenmodell der Lebermetastasen bei Kolorektalkarzinom untersucht. Die Tiere wurden, nach der Induktion von Lebermetastsen des Kolorektalkarzinoms, mit dem FOLFOX Schema ± 5% Glycin haltigem Futter therapiert. Die Tumoren wurden mittels µCT Scans der Leber und immunhistochemischem Nachweises von Ki67 und CD31 charakterisiert. Weiters wurde die linksventrikuläre Auswurffraktion (LVEF), die myokardiale Fibrose und Apoptose, sowie die Levels des heart fatty acid-binding protein (h-FABP), und brain natriuretic peptide (BNP) monitorisiert. Die Expression von Kollagen Typ I, II und BNP im Herzmuskel wurde mittels qPCR analysiert. Glycin zeigte keinerlei Effekte im Hinblick auf Zellviabilität in den in vitro Versuchen sowohl mit CC531 als auch mit HCM Zellen. Hingen zeigten die in vivo Untersuchungen, dass Glycin Supplementierung die Dichte der Tumor Mikrovaskulatur (MVD) signifikant, um 60%, verringert ($p=0.004$) und das Tumorvolumen auf 42-35% vom Volumen der Kontrollen ($p<0.05$) verringert. Zusätzlich

beeinträchtigte Glycin die anti-tumor Eigenschaften der Chemotherapie nicht. Wie erwartet stiegen mit Verabreichen der FOLFOX Therapie die h-FABP Levels, die myokardiale Fibrose, Apoptose und die Expression des Typ I Kollagens signifikant an. Weiters wurde die LVEF signifikant, um 10%, reduziert (p=0.028). Glycin war in der Lage dem Chemotherapie-induzierten myokardialen Schaden, durch Reduktion des Fibrosegrades (p=0.012) und der Apoptosen (p=0.015) sowie Erhaltung der LVEF vorzubeugen. Diese Arbeit konnte zeigen, dass die Supplementierung von Glycin das Wachstum von Lebermetastasen des Kolorektalkarzinoms verringert, ohne die Wirkung von FOLFOX zu beeinträchtigen und gleichzeitig die FOLFOX induzierten Herzschädigung unterbindet. Der zugrundeliegende Mechanismus ist möglicherweise die Verringerung der MVD. Um Glycin erfolgreich in die FOLFOX Therapie der Lebermetastasen bei Kolorektalkarzinom einbinden zu können, sind jedoch weiterführende klinische Studien notwendig.

Abstract in English

Globally colorectal cancer is among the most prevalent cancers affecting more than 1.8 million people each year. About every second patient is diagnosed with distant metastases through the course of the disease and liver metastases are the most common site of distant spread. Systemic chemotherapy, such as FOLFOX, is indicated before surgical resection to improve long-term outcomes or achieve resectability. However, chemoresistance and chemotoxicity may limit treatment efficacy. Side effects including rare, but potentially lethal and currently unavoidable cardiotoxicity have to be avoided.

Previously glycine has been suggested to have anti-tumorigenic properties in several types of cancer. Further, glycine has other biological actions including an inhibitory effect on platelet aggregation, hepatoprotective and antioxidative properties. Also, it has been shown to improve microperfusion. Thus, this study was conducted to test whether dietary glycine together with conventional FOLFOX chemotherapy in colorectal cancer liver metastases is oncological effective and has cardioprotective properties against chemotherapy-induced cardiotoxicity. The glycine effect was evaluated in vitro on colorectal cancer cells (CC531) and human cardiac myocytes (HCMs). To investigate the glycine effect in vivo, Wag/Rij rats with induced colorectal cancer liver metastases were treated with FOLFOX±5% dietary glycine. The tumors were characterized by µCT liver scans as well as immunohistochemistry including anti-Ki67 and anti-CD31 stainings. Heart fatty acid-binding protein (h-FABP) and brain natriuretic peptide (BNP) levels, left ventricle ejection fraction (LVEF), myocardial fibrosis, and apoptosis, were evaluated. Expression of BNP and collagen type I and II in cardiac muscle was analyzed by qPCR. The results of the study did not show any effects of glycine on CC531 and HCM viability in vitro. However, in vivo, glycine significantly decreased tumor microvascular density (MVD) by 60% ($p=0.004$) and tumor volume to 42-35% of that of controls ($p<0.05$). Furthermore, glycine did not hinder the anti-tumorigenic properties of chemotherapy. As expected, FOLFOX significantly increased myocardial fibrosis and apoptosis, h-FABP levels also the expression of the type I collagen gene. It also significantly impaired LVEF by 10% ($p = 0.028$). Glycine prevented chemotherapy-induced myocardial injury by reducing fibrosis degrees ($p = 0.012$) and apoptosis ($p=0.015$), and by preserving LVEF. Therefore, this study provided evidence that glycine suppresses the growth of colorectal cancer liver metastases without impairing the effectiveness of

conventional FOLFOX chemotherapy and prevents FOLFOX-induced heart injury. Glycine's antitumorigenic activity most likely includes antiangiogenic action to decrease tumor MVD. Clinical studies are necessary to implement glycine into FOLFOX treatment for colorectal cancer liver metastases.

1. Introduction

1.1. Colorectal cancer: epidemiology

Colorectal cancer (CRC) is the 3rd most common and 2nd most deadly cancer worldwide. More than 1.9 million new cases and more than 900 thousand deaths were estimated to occur in 2020 (Arnold et al., 2017; Bray et al., 2018; Sperling et al., 2013; Sung et al., 2021; Torre et al., 2015). Alarmingly, CRC incidence is anticipated to increase in the nearest future. More than 2.5 million cases are expected to be diagnosed in 2035 (Dekker et al., 2019). CRC incidence in males is approximately 25 % higher than in females and mortality rates as well (Dekker et al., 2019). These rates also vary geographically, with up to 8-fold differences between countries (Rawla et al., 2019). The highest incidence is observed in high-income regions such as Europe, North America, and Australia while the lowest incidence is seen in South-Central Asia and Africa (Haggar and Boushey, 2009; Rawla et al., 2019). Such discrepancies have been primarily attributed to the availability of modern healthcare, including nationwide screening programs and utilization of colonoscopies (Dekker et al., 2019). Although differences in lifestyle and dietary habits may also play a role (Dekker et al., 2019). CRC can develop at any age, but elderly people are at higher risk. The median age at the diagnosis of CRC is about 70 years (Brenner et al., 2014). However, a worrying rise of CRC in young patients (< 50 years) has been noticed recently, especially left colon and rectal cancer (Dekker et al., 2019). While genetic, lifestyle and environmental factors are possible explanations, the exact cause for this phenomenon remains unrecognized (Dekker et al., 2019).

1.2. Colorectal cancer: risk factors, pathogenesis, and development of the disease

CRC is multifaceted and composed of lifestyle, genetic, and some environmental factors (Aran et al., 2016). Both non-hereditary and hereditary CRC types exist, but the majority are non-hereditary cases triggered by somatic mutations induced by environmental factors (Aran et al., 2016). Some of the risk factors for CRC are well described in the current literature. These include hereditary CRC syndromes, positive family history, male gender, type 2 diabetes, history of inflammatory bowel diseases, obesity, smoking, consumption of red or processed meat, high/moderate alcohol intake, and low fruits and vegetables consumption (Dekker et al., 2019; Simon, 2016). On the contrary, among others, some dietary products (fibers, whole grains, fish, dairy products, and vitamins), physical activity, menopausal hormone therapy, and some drugs (statins and aspirin) reduce the risk of CRC development (Dekker et al., 2019; Simon, 2016).

Most CRCs arise from pre-cancerous polyps that are broadly categorized as either traditional tubular adenomas or serrated polyps (Nguyen et al., 2020). This long-lasting process typically takes about 10–15 years. The process starts with an aberrant crypt transforming to a polyp (neoplastic precursor lesion) which finally progresses to CRC (Dekker et al., 2019). Currently, it is believed that the majority of CRCs originate from stem cells or stem-cell-like cells (Dekker et al., 2019; Medema, 2013; Nassar and Blanpain, 2016). The development of these cancer stem cells is a consequence of different genetic and epigenetic changes which inhibit tumor-suppressor genes and activate oncogenes (Dekker et al., 2019).

DNA mutations may be inherited or acquired (Simon, 2016). Truly inherited mutations linked with CRC, such as MLH1, MSH2, PMS2, and APC gene mutations are rare and only account for ~5 % of CRCs (Simon, 2016). However, recognizing these inherited changes in the setting of sporadically occurring APC and DNA mismatch repair mutations helps explain the stepwise genetic progression from benign polyps to CRC (Simon, 2016). There are two major precursor lesion pathways: 1) traditional adenoma-to-carcinoma pathway accounting for up to 90 % of CRCs and 2) serrated neoplasia pathway accounting for up to 10 % of cases (Dekker et al., 2019). These pathways present different epigenetic and genetic actions in sequential order ("Comprehensive molecular characterization of human colon and rectal cancer," 2012; Dekker et al., 2019). Conventional adenomas progress by the accumulation of genetic mutations causing chromosomal instability and leading to microsatellite-stable tumors. Usually, the initial genetic mutations are within the APC gene resulting in defective chromosome segregation at cell division phase (Dekker et al., 2019; Simon, 2016). Subsequent mutations then evolve in the KRAS and/or BRAF oncogenes which over time can promote a loss of TP53 gene function. This major regulator of transcription and apoptosis impacts cellular functions which ultimately result in carcinogenesis (Dekker et al., 2019; Simon, 2016). Conversely, the serrated neoplasia pathway is frequently initiated by mutations of KRAS or BRAF genes, and epigenetic instability characterized by the CpG island methylation, resulting in microsatellite unstable and stable cancers (Dekker et al., 2019). Another mechanism contributing to the genetic diversity of CRCs is microsatellite instability (MSI), which is triggered by defective repair of DNA due to the inactivation of mismatch repair genes. MSI can take place in both serrated and adenomatous polyps (Dekker et al., 2019; Simon, 2016).

Following initial formation, the tumor grows to a size of approximately 1–2 mm^3 after which its' metabolic demands are confined by the limit of the diffusion process to supply a sufficient amount of nutrients and oxygen (Hillen and Griffioen, 2007). To grow further, the tumor becomes angiogenic and utilizes vasculature from the surrounding stroma (Hillen and Griffioen, 2007). Angiogenesis typically begins at the capillaries and has a key role not exclusively in local tumor growth but also in the processes of metastasis development (Lugano et al., 2020). As capillaries develop within the tumor and malignancy progresses, cells enter the circulation via microinvasion (Manne et al., 2010). Although microinvasion begins in most adenomas, metastasis remains unlikely (Manne et al., 2010). This is either because the volume of malignant cells is low or because only a limited number of neoplastic cells are exposed to lymphatic vessels, which are rare in colorectal mucosa (Manne et al., 2010), and mainly found at the base of the mucosa and in the lamina propria (Manne et al., 2010). As the tumor grows and invades deeper layers of the intestinal wall, the cancer cells interact with a greater number of lymphatics and blood vessels, therefore tumor metastatic potential increase (Manne et al., 2010). This leads to a greater likelihood of metastatic spread to local lymph nodes and/or distant metastases (Manne et al., 2010). Alternatively, the metastatic potential could be mediated by metastasis-inducing genes, such as osteopontin, MEK1, and CXCR4 (Manne et al., 2010; Richert et al., 2009). About two-thirds of CRC patients will be diagnosed with distant metastasis throughout the course of their disease (Kow, 2019). The most common site of metastases is the liver, followed by the lung, peritoneum, and then other sites such as bone, spleen, brain, and others (Disibio and French, 2008; Hess et al., 2006; Hugen et al., 2014; Kow, 2019; Riihimäki et al., 2016; Weiss et al., 1986).

1.3. Colorectal cancer: current treatment standards and outcomes

Surgery remains the main treatment option for early and locoregionally advanced CRC (Dekker et al., 2019). Modern surgical options include endoscopic, laparoscopic, robotic, and conventional open surgery. Upfront surgery is the standard for resectable colon cancer. Similarly, early rectal cancer can be managed by surgical removal, although neoadjuvant radiotherapy or chemoradiotherapy is indicated for locally advanced middle or lower rectal cancer (Argilés et al., 2020; Glynne-Jones et al., 2017). After resection, the surgical specimen has to be carefully evaluated by an experienced pathologist as suggested by the European Society for Medical Oncology (Argilés et al., 2020; Glynne-Jones et al., 2017), and the pathological stage and tumor characteristics must be determined. The indications for adjuvant chemotherapy should be considered in each individual case. Definitive decisions regarding adjuvant treatment are made after discussing the risks and benefits with patients. Ultimately, the risk of tumor recurrence must be considered in relation to the expected benefits and complications of adjuvant treatment (Argilés et al., 2020; Glynne-Jones et al., 2017).

Treatment strategy for metastatic CRC depends on tumor burden. Only a limited proportion of patients present with metastatic disease that is suitable for potentially curative resection at initial diagnosis (Cutsem et al., 2014). In patients with initially unresectable metastases, a subgroup may become suitable for resection after a major response to conversion chemotherapy (Cutsem et al., 2014). The optimal treatment strategies for patients with clearly unresectable metastatic CRC are rapidly evolving (Cutsem et al., 2014). The treatment goals of these patients should include prolonging survival, addressing tumor-related symptoms, and stopping tumor progression to maintain quality of life (Cutsem et al., 2014). Most recently, there has been increasing evidence that ablative therapy may have a role for these patients, even if resectability is not achieved following initial systemic treatment (Cutsem et al., 2014).

The prognosis of CRC patients has slowly but steadily improved during the last decades (Brenner et al., 2014). Five-year relative survival has reached almost 65 % in high-income countries; although it remains less than 50% in low-income countries (Brenner et al., 2014). The stage of disease at the time of diagnosis remains the strongest prognostic factor (Brenner et al., 2014). Five-year relative survival for patients diagnosed with locoregional CRC, when surgery can still be a radical treatment, is about 90–70 % (Brenner et al., 2014). In contrast, this number is less than 15 % in patients with distant tumor spread (Brenner et al., 2014).

1.4. Colorectal cancer: treatment of colorectal cancer liver metastases

Up to 55 % of CRC patients will develop colorectal cancer liver metastases (CRLM) throughout the course of the disease, thus the liver is the most common site of metastasis (Akgül et al., 2014; Al Bandar and Kim, 2017; Vatandoust et al., 2015; Zervoudakis et al., 2017). Resection of CRLM may be a curative option, although the majority (~85 %) of patients are initially unresectable (Sanoff et al., 2008; Zervoudakis et al., 2017). In these cases, chemotherapy (CTx) is used to improve the chances of resectability or to control the disease (Maneikyte et al., 2019). FOLFOX regimen (5-fluorouracil (5-FU), oxaliplatin (OX), leucovorin), with or without different monoclonal antibodies targeting against vascular endothelial growth factor (VEGF) or epidermal growth factor receptor (EGFR), is today's standard for CRLM (Maneikyte et al., 2019). Despite the most modern CTx, a substantial percentage of CRC patients still face chemoresistance leading to treatment failure (Fang et al., 2015; Toden et al., 2015). Furthermore, the use of conventional cytotoxic and cytostatic agents such as 5-FU and OX is associated with numerous side effects including hematological toxicity, gastrointestinal toxicity, hepatotoxicity, neurotoxicity, kidney injury, cardiotoxicity, and others (Cassidy et al., 2008; Munker et al., 2018). Cardiotoxicity is not common, but a potentially lethal complication of FOLFOX (de Forni et al., 1992; Maneikyte et al., 2020). The reported rate of 5-FU-induced cardiotoxicity range between 1% and 68% for different solid cancers (Labianca et al., 1982; Rezkalla et al., 1989; Yeh and Bickford, 2009), with 8.5% rate in specific CRC patients cohort (Jensen et al., 2010). Such chemotherapy-related adverse events lead to deterioration in the quality of life, inadequate treatment, and higher medical costs (Maneikyte et al., 2019; Vogel et al., 2017). Thus, there is a need for novel anti-cancer agents and preventive strategies against CTx-induced cardiotoxicity.

1.5. FOLFOX induced cardiotoxicity

The exact pathological mechanisms for FOLFOX-induced cardiotoxicity remain unclear but it is known that both agents—5-FU and OX— may have cardiotoxic properties. Different pathomechanisms such as arteritis, coronary thrombosis, and vasospasm have been suggested (Madeddu et al., 2016; Maneikyte et al., 2020). Current evidence also describes a straight 5-FU-induced cytotoxic impact on the endothelial cells which results in the release of various vasoactive substances causing a prothrombogenic state (Batta H. Abd El Azim, n.d.; Maneikyte et al., 2020). Also, there is some evidence for the direct toxic injury of cardiomyocytes by 5-FU. Also, its impact on the coagulation system, and mechanisms related to autoimmune responses (Madeddu et al., 2016; Maneikyte et al., 2020). Pathological mechanisms for platinum-based drugs' cardiotoxicity remain obscure as well (Maneikyte et al., 2020; Oun et al., 2018). The existing hypotheses include secondary toxic effects because of nephrotoxicity, potentially negative effects on the sinoatrial node, and straightforward cellular damage via reactive oxygen species-mediated mechanisms (Maneikyte et al., 2020; Oun et al., 2018; Oun and Rowan, 2017). Furthermore, the combination of OX and 5-FU seems to increase the incidence of cardiotoxicity (Kwakman et al., 2017; Maneikyte et al., 2020; Morrow and Hoff, 2006).

Besides polychemotherapy, other risk factors for fluoropyrimidine-induced cardiotoxicity include frequency of administration, previous radiotherapy, and other concurrent cardiovascular diseases (Layoun et al., 2016). Traditionally the continuous infusion of 5-FU, as it is in FOLFOX for CRLM, has been the preferred option for administration because of increased efficacy and lower toxicity (Layoun et al., 2016). However, recent evidence shows that continuous 5-FU infusion is related to an increased risk of cardiotoxicity compared to the bolus infusion, suggesting that prolonged exposure to 5-FU can be harmful (Layoun et al., 2016). Another risk factor for cardiotoxicity is the previous radiotherapy to the chest wall, especially if doses were higher than 30–35 Gy (Layoun et al., 2016). Existing cardiovascular comorbidities, such as ischemic coronary disease or structural heart diseases are linked to a several-fold increased risk for 5-FU cardiotoxicity (Layoun et al., 2016).

Management of cancer patients with suspected fluoropyrimidine-induced cardiotoxicity includes a multidisciplinary approach between cardiologists and oncologists, and immediate discontinuation of the chemotherapy (Layoun et al., 2016). Before restarting chemotherapy, alternative drugs of different classes should be considered (Layoun et al., 2016). If no alternative for 5-FU exists, coronary angiography may be considered and cardiovascular disease-related biomarkers should be evaluated to stratify risk (Layoun et al., 2016). As pre-existing cardiovascular diseases and its' associated risk factors increase chances of cardiotoxicity, they must be addressed. Efficient arterial blood pressure control, use of statins, smoking cessation, and efficient control of diabetes have to be ensured before restarting 5-FU (Layoun et al., 2016).

Currently, there is no strong evidence for efficient pharmacological prophylaxis to prevent 5-FU-induced cardiotoxicity (Layoun et al., 2016). Beta-blockers, calcium channel blockers, and long-acting nitrates, have been trialed, although, none of the studies provided definitive conclusions (Collins and Weiden, 1987; Layoun et al., 2016; Oleksowicz and Bruckner, 1988; Polk et al., 2013; Schöber et al., 1993). Innovative agents like a piperazine derivative - ranolazine, used to treat refractory angina, are under investigation in the current INTERACT trial, although, the results are still pending (Minotti, 2013). Thus, there is a critical need for efficient and novel preventive strategies, because myocardium injury at FOLFOX-induced cardiotoxicity can be irreversible and even lead to death.

1.6. Glycine

The smallest amino acid – glycine, consists of a carbon molecule connected to an amino and a carboxyl group (Hall, 1998). Traditionally, glycine was considered a non-essential amino acid, because of its endogenous synthesis (Wu, 2010). Although current evidence suggests that in vivo synthesized amount of glycine is not enough for metabolic demands and thus is a conditionally essential amino acid (Wang et al., 2013). Glycine has important physiological functions and plays a substantial role in metabolism. It represents 20 % of amino acid nitrogen in body proteins and 11.5 % of total amino acids (Wang et al., 2013). Glycine is a major compound in proteins of extracellular structures such as elastin and collagen (Wang et al., 2013). Glycine is also crucial for the synthesis of creatine, purines, serine, glutathione, and heme (Hall, 1998). These substances participate in muscle and nerve energy metabolism, antioxidative intracellular systems, DNA and protein synthesis, cell proliferation, and oxygen transport (Wang et al., 2013). Also, glycine plays a crucial role in the conjugation of bile acids, thereby aiding digestion and absorption of lipids and lipid-soluble vitamins (Wang et al., 2013). Glycine regulates calcium influx through glycine-gated chloride channels in immune cells, resulting in the production of cytokines and the generation of superoxide; both of which regulate immune function (Belachew et al., 2000; Wang et al., 2013). In the central nervous system, glycine acts as a neurotransmitter hence affecting food intake, behavior, and whole-body homeostasis (Wang et al., 2013). Therefore, glycine has broad functions and is essential in physiology. It plays a part in growth and development, metabolism, immunity, cytoprotection, and ultimately the survival of animals and humans (Wang et al., 2013).

1.7. Glycine impact on ischemia-related injury

The drugs that cause vasoconstriction or disturb mitochondrial function, as is proposed for 5-FU-induced cardiotoxicity (Madeddu et al., 2016; Maneikyte et al., 2020), can induce ischemia or ischemia-like injury (Zhong et al., 2003). Various conditions are associated with ischemia-reperfusion injury including major surgery or transplantation, stroke, hemorrhagic shock, and cardiovascular diseases (Madeddu et al., 2016; Maneikyte et al., 2020). Glycine may directly protect cells against such hypoxic insult in the ischemic phase, by protecting plasma membrane integrity (Marsh et al., 1993; Qian et al., 1997; Venkatachalam et al., 1996; Zhong et al., 2003). Furthermore, glycine prevents tissue damage and stunts inflammatory responses in the reperfusion phase. It hinders activation of neutrophils and macrophages, production of toxic mediators and free radicals, and activity of some degradative enzymes such as proteases (Zhong et al., 2003). The positive effect of glycine was shown in a series of experimental ischemia-reperfusion and transplantation models. Local tissue perfusion with 20 % glycine in the pre-ischemia or pre-reperfusion phase increased the mucosal protein and DNA content, decreased myeloperoxidase activity, and increased activity of glutaminase in the small bowel ischemia-reperfusion model (Lee et al., 2002). Perfusion with 2.2 % of glycine solution decreased muscle edema, necrosis, preserved muscle function, and energy stores in a skeletal muscle ischemia-reperfusion canine model (Ascher et al., 2001). Glycine as an additive to preservation solutions or as a substance in donor preconditioning improved liver transplantation outcomes by prolonging graft survival and preventing hepatocellular injury, by increasing sinusoidal blood flow, decreasing leukocyte-endothelium interactions, and slowing Kupffer cell-derived TNF-α production (Al-Saeedi et al., 2019; den Butter et al., 1993; Schemmer et al., 1999a). Furthermore, intravenous glycine diminished MPO and pancreatic cytokines activity, reduced necrosis, and decreased inflammatory cell infiltration in the experimental acute pancreatitis model (Ceyhan et al., 2011). All of these findings support glycine as an effective substance against ischemia-reperfusion or ischemia-like injury.

1.8. Glycine against platelet aggregation

Experimental and clinical observations have described thrombotic states in various cardiovascular diseases (Becker, 1991; Gori, 2011; Schemmer et al., 2013), including hypercoagulability leading to thrombosis in 5-FU induced cardiotoxicity (Sara et al., 2018). Platelet thrombus formation is an essential physiologic process that facilitates hemostasis (Ruggeri, 1997). However, when the pathway is dysregulated it can lead to unwanted thrombotic occlusion of vessels compromising blood flow to vital organs (Ruggeri, 1997). Intracellular calcium ($[Ca^{2+}]_i$) is a key regulator of platelet function (Dolan and Diamond, 2014). A rise in $[Ca^{2+}]_i$ activates actin cytoskeleton reorganization and degranulation or inside-out activation of integrin αIIbß3, which are crucial for platelet aggregation (Varga-Szabo et al., 2009). The levels of $[Ca^{2+}]_i$ increase from two major sources: 1) the release of compartmentalized Ca^{2+} and 2) the entry of extracellular Ca^{2+} through the plasma membrane (Varga-Szabo et al., 2009). Glycine can prevent an agonist-induced intracellular influx of calcium by binding on its receptor (GlyR) and stimulating Cl^- influx that causes membrane hyperpolarization (Schemmer et al., 2013). Different blood cells including platelets contain these GlyR (Ikejima et al., 1997; Schemmer et al., 2013; Wheeler et al., 2000, 1999). Hence, glycine reduces platelet aggregation and diminishes thrombotic risk. It has been shown that dietary glycine increases plasma glycine levels, inhibits ADP or collagen-stimulated platelet aggregation, and significantly increases bleeding time in rats (Schemmer et al., 2013). Similarly, glycine has also been demonstrated to blunt aggregation of human platelets in a dose-dependent manner via mechanisms involving the glycine receptor (Schemmer et al., 2013).

1.9. Antitumorigenic properties of glycine

The non-toxic amino acid glycine (Bruns et al., 2016; Evins et al., 2000; Gannon et al., 2002; Kaufman et al., 2009) has anti-tumorigenic properties as shown by several previous pre-clinical studies (Rose et al., 1999b, 1999a). Rose et. al demonstrated that a 5 % glycine-enriched diet reduced melanoma growth by 50-75 % in C57BL/6 mice (subcutaneous tumor model) by reducing tumor vessel density (Rose et al., 1999b). Another study showed that 5 % dietary glycine did not inhibit hepatocarcinogenic WY-14,463-induced liver cancer formation, but it did significantly decrease tumor progression (Rose et al., 1999a). Further experiments with a 5 % glycine-enriched diet showed that it can also decrease CRC growth by ~65 % and reduce peritumoral microvessel density in rats (Bruns et al., 2016). The 5 % glycine diet used in these experiments is standard in such studies and usually increases serum glycine levels to about 1 mM (Bruns et al., 2016). In vitro, 1mM glycine blunts VEGF stimulated human umbilical vein endothelial cell (HUVEC) growth, migration, and angiogenesis (Bruns et al., 2016). Glycine's anti-angiogenic effect may be neutralized by strychnine, a competitive antagonist to glycine receptors. Thus there is some indirect evidence that GlyR mediates the anti-angiogenic mechanism of glycine (Bruns et al., 2016). Similar properties were demonstrated in an experimental study by Bruns et al. (Bruns et al., 2014). Although different concentrations of glycine did not have direct pro- or antiproliferative effects upon hepatocellular carcinoma cells (HepG2 and Huh7), it did significantly decrease VEGF-A expression on both - mRNA and protein levels in both cell lines (Bruns et al., 2014). The study concluded that glycine decreases VEGF-A-mediated angiogenic signalling via GlyR-dependent pathways in human HCC. Therefore, glycine was hypothesized to be a promising conjunct to chemotherapy treatment for different highly vascularized tumors.

On the contrary, there is some discussion that glycine itself may have a pro-tumorigenic effect as well. A recent study performed metabolite profiling and suggested glycine has a major role in rapid proliferation of cancer cells. Thus, the metabolism of glycine was suggested as a potential target for therapy (Jain et al., 2012; Maneikyte et al., 2019). Moreover, the restriction of dietary glycine and serine was shown to effectively decrease CRC growth in a mouse model (Maddocks et al., 2017; Maneikyte et al., 2019). Contrary, extensive cellular-level investigations of glycine and serine role in proliferation and metabolism of cancer cells did not show that restriction of exogenous glycine or depletion of the glycine cleavage system impedes proliferation of cancer cells (Labuschagne et al., 2014; Maneikyte et al., 2019).

Glycine may affect CRC progression in multiple ways since it has immunomodulatory effects and can contribute to both a local and widespread response to CRC (Wheeler et al., 1999; Zhong et al., 2003). Conventional chemotherapy, such as FOLFOX, also modulates immune response (Guan et al., 2020; Maeda et al., 2011), hence its interaction with glycine may have unexpected outcomes. These questions remain to be elucidated in future in vivo studies before wide-scale clinical trials can be justified.

1.10. Glycine against chemotherapy and other drugs induced toxicity

Besides antitumorigenic properties, glycine may have a beneficial effect against chemotherapy-induced organ toxicity. Previous studies have shown protection from substance and drug-induced liver or kidney injury (Zhong et al., 2003). Mechanisms of protection vary and depend on the type of toxicants (Zhong et al., 2003). For example, cyclosporin A, the widely used immunosuppressant, has multiple toxic effects, including nephro- and hepato- toxicity (Zhong et al., 2001, 1999). The risk of both can be decreased by dietary glycine (Zhong et al., 2001, 1999). Cyclosporin A also induces a hypermetabolic state and causes hypoxia in liver tissue, which inhibits liver function. Glycine is thought to provide protection by inhibition of Kupffer cells (KCs) (Zhong et al., 2003, 2001). Glycine's inhibition of KCs is also important for the hepatoprotective effect against FOLFOX-induced liver injury as shown in a recent study (Mikalauskas et al., 2011). Cytotoxic chemotherapy agents, like many other drugs or toxicants, activate KCs by inducing a hypermetabolic state and causing hypoxia in liver tissue (Mikalauskas et al., 2011; Zhong et al., 2003). The active KCs impair hepatic microcirculation by releasing vasoactive mediators and therefore form a vicious circle of further hypoxia, cellular damage, and further KC activation (Mikalauskas et al., 2011). Additionally, active KCs produce hepatotoxic molecules such as reactive oxygen and nitrogen species (Mikalauskas et al., 2011). Glycine prevents activation of KCs and thus improves hepatic microperfusion. This decreases the risk of liver injury as shown in previous chemotherapy- and non-chemotherapy-induced hepatotoxicity in-vivo models (Mikalauskas et al., 2011; Rivera et al., 2001; Schemmer et al., 1999b, 1998).

Another phenomenon in the early stages following chemotherapy application is white blood cells adherence to endothelium and their activation leading to the release of cytotoxic mediators (Mikalauskas et al., 2011). As previously noted, glycine improves intrahepatic microcirculation preventing cell adhesion to the endothelium and protecting hepatocytes from cytotoxic injury (Mikalauskas et al., 2011). Such hepatoprotective properties of glycine make it an appealing substance to use in studies aimed at reducing the side effects of conventional chemotherapy.

1.11. Safety of glycine in a clinical setting

Until today different indications for glycine as a supplement use have been established in clinical practice. For example, its' solution is used for local irrigation during transurethral urine bladder or prostate resections, for total parenteral nutrition, and some others (Luntz et al., 2005). Glycine has also been investigated in several clinical trials in psychiatry (Evins et al., 2000) and transplant medicine (Luntz et al., 2005). For example, up to sixty grams of dietary glycine administered daily for 8 weeks have shown no serious toxicities (Evins et al., 2000). Such treatment increased glycine concentration in plasma from physiological levels to up to 1.3 mM. This concentration exceeds the commonly used and effective serum level of ~1 mM in preclinical models (Bruns et al., 2016). Furthermore, glycine is released at the digestion of protein, and even high doses of it are considered non-toxic (Zhong et al., 2003). However, there is a report suggesting that glycine may be toxic and even lead to cardiac arrest and death (Byard et al., 2001). In that case, a 69-year-old man underwent transurethral prostate resection and cystolithopexy for benign hyperplasia using glycine irrigation fluid (Byard et al., 2001). Following the procedure, the posterior bladder wall was injured and the irrigation solution leaked to the retroperitoneum (Byard et al., 2001). Despite urgent laparotomy and retroperitoneal fluid evacuation, cardiac arrest occurred during the surgery and resuscitation was unsuccessful. The autopsy demonstrated hyponatremia with significantly increased levels of urine, blood, and body fluid glycine levels. Therefore, death was attributed to glycine toxicity (Byard et al., 2001). The potential cardiotoxicity of glycine was also described in a preclinical model after intravenous infusion of a high dose of glycine (1.5%, 300 ml/kg body weight) (Olsson and Hahn, 1999). However, such dose is approximately 50-fold higher compared to those used in a majority of studies showing protective effects of glycine in experimental animals or humans (Zhong et al., 2003). As glycine at high-dose may have a toxic effect, further studies for safe doses and routes of administration are needed. Although to date, there is evidence that up to 60 g of dietary glycine can be administered safely and such dose can increase the plasma glycine levels above 1mM.

1.12. The gap of current knowledge and the aim of the current study

Glycine seems like a promising additive to conventional chemotherapy (i.e. FOLFOX) for CRLM because of its known antitumorigenic and organ protective properties as stated above. Furthermore, glycine is non-toxic and available to use in a clinical setting. Although there are no in-vivo studies investigating glycine efficacy when combined with FOLFOX, preclinical studies are necessary before initial clinical trials could be initiated. Thus, this study aimed to investigate the effects of glycine in combination with FOLFOX in CRLM treatment both in vivo and in vitro. Also, the study aimed to investigate the cardioprotective potential of glycine in a model of rats suffering from CRLM and treated with a single cycle of FOLFOX.

2. Material and Methods

The description of some parts of the Material & Methods section may be similar to those published previously by *Maneikyte et al.; 2019* (Maneikyte et al., 2019) and *Maneikyte et al.; 2020* (Maneikyte et al., 2020).

2.1. Cell culture experiments

2.1.1. Cell lines and viability testing

For experiments two different cell lines: 1) rat colon adenocarcinoma cell line CC-531 (CC531) (Cell Lines Service, Eppelheim, Germany) and 2) human cardiac myocytes (HCMs, Promo Cell, Heidelberg, Germany) were cultivated in a humidified atmosphere with 5% CO_2 at 37 °C. Standard RPMI-1640 medium supplemented with 10% fetal bovine serum (GE Healthcare Life Sciences, Utah, USA), 1% L-glutamine, 25mM HEPES, and 1% penicillin/streptomycin (Maneikyte et al., 2019) and ready-to-use Myocyte Growth Medium (Promo Cell, Heidelberg, Germany) was used for CC-531 and HCMs, respectively. The medium was renewed every second/third day and cells were re-seeded after 90% confluence was achieved (Maneikyte et al., 2020).

To test the cell viability the 3-(4,5-dimethylthiazol-2-yl)5-diphenyltetrazolium bromide (MTT; Sigma Aldrich, St. Louis, MO, USA) assay was performed as described in the manufacturer's instructions. Shortly, ten microliters of MTT (Sigma Aldrich, St. Louis, MO, USA) were added to cells, and the solution was incubated at 37°C for 2 hours. After, the medium was discarded, and the precipitated formazan crystals were dissolved in dimethyl sulfoxide (DMSO; Sigma Aldrich, St. Louis, MO, USA). After 30 minutes of resting at room temperature plates were put into a Spectroxtar microplate reader (BMG labtech, Ortenberg, Germany) and optical density was measured at 570 nm. All experiments were performed in duplicates and repeated three times. Cell viability was calculated as a percentage of vehicle control. (Maneikyte et al., 2020, 2019).

2.1.2. Glycine impact on cell lines

To define glycine impact on CC531 and HCMs, they ($5x10^3$ CC531; 1.5×10^4 HCM) were seeded in 96-well plates with glycine-free media and incubated for 24h under standard laboratory conditions. After media was supplemented with different concentrations of glycine (Control (0), 0.05, 0.1, 0.25, 0.5, 1, 2, 4, and 8 mmol/L; Carl Roth, Karlsruhe, Germany), cells were grown for additional 48 hours. After such conditioning, the MTT test was performed as described above to assess cell viability (Maneikyte et al., 2019).

2.1.3. Glycine in combination with 5-fluorouracil and oxaliplatin

To evaluate conventional chemotherapy agents - 5-FU and OX - interaction with glycine CC531 cells were treated with a drug cocktail for 48 hours. The cocktail consisted of 5-FU or OX at the half-maximal inhibitory concentration (IC50) mixed with different concentrations (from 0.1 to 5 mM) of glycine. After, MTT assay was performed as described above to test cell viability. The IC50 was determined from the dose-response curves obtained from the MTT test after CC531 cells were treated for 48-h with 1 to 800 µM 5-FU or OX (Maneikyte et al., 2019).

2.2. Animal experiments

2.2.1. Ethics and experimental animals

Before the start of the animal experiments approval from Republic of Austria federal ministry of education, science, and research (BMWFW-66.010/0130-WF/V/3b/2017) was obtained. Austrian national laws and 3Rs principles (Replacement, Reduction, and Refinement) for animal care in scientific research were followed through all in vivo experiments.

For the study 7-week-old male Wag/Rij rats weighing 150 - 220 g were purchased from Charles River company (Wilmington, MA, USA). After delivery rats were kept under standard laboratory conditions with a 12:12 h light:dark cycle in the animal facility of Medical University of Graz. All experimental animals had no restrictions for access to water and food. After 7 days of acclimatization experiment started. Weighing and blood drawing was done on the 1^{st}, 6^{th}, 14^{th}, 17^{th}, and 21^{st} days of the experiment. All study-related interventions in animals were performed at approximately the same daytime to avoid potential natural circadian rhythms causing bias.

2.2.2. Experimental protocol

Figure 1 shows the study design. On day 1 experiment started by randomizing experimental animals (n=44) into 6 groups and changing regular rat chow to study diets. Twenty-two rats received a 5% glycine-enriched diet (glycine diet: modified C1000 diet 15% casein plus 5% glycine; Altromin Spezialfutter, Lage, Germany). Other rats (n = 22) received a 20% casein diet (control diet: 20% casein; Altromin Spezialfutter, Lage, Germany) which was chosen as a control diet to maintain isonitrogenous balance. This casein diet is a standard control for dietary glycine in an experimental setting (Mikalauskas et al., 2011). On day 6 CRLM were induced by injecting CC531 cells in the right liver lobe (for details of the procedures see below). Animals in Casein-Sham (n=4) and Glycine-Sham (n=4) groups received a similar procedure, but with an injection of cell-free PBS. On day 14 ɥCT was performed to measure tumor volume and heart ultrasound to evaluate heart function for all animals (for details of the procedures see below). Just after radiological imaging tests animals were treated with a single cycle of FOLFOX CTx. It consisted of 200 mg/m^2 calcium folinate (Sandoz, Holzkirchen, Germany), 85 mg/m2 OX (Fresenius Kabi, Bad Homburg, Germany) and 1000 mg/m^2 5-FU (Sandoz, Holzkirchen, Germany) applied intraperitoneally and additional 200 mg/m^2 calcium folinate and 1000 mg/m^2 5-FU applied the same way after 24 hours. Animals' skin surfaces were used to estimate drug doses (Mikalauskas et al., 2011). Animals from Casein-Sham, Glycine-Sham, Casein-Control, and Glycine-Control groups received an equivalent volume of 0.9 % NaCl solution. On day 21, ɥCT and heart ultrasound were repeated for tumor volume and heart function evaluation. Afterward, animals were sacrificed for tissue and blood collection (Maneikyte et al., 2020).

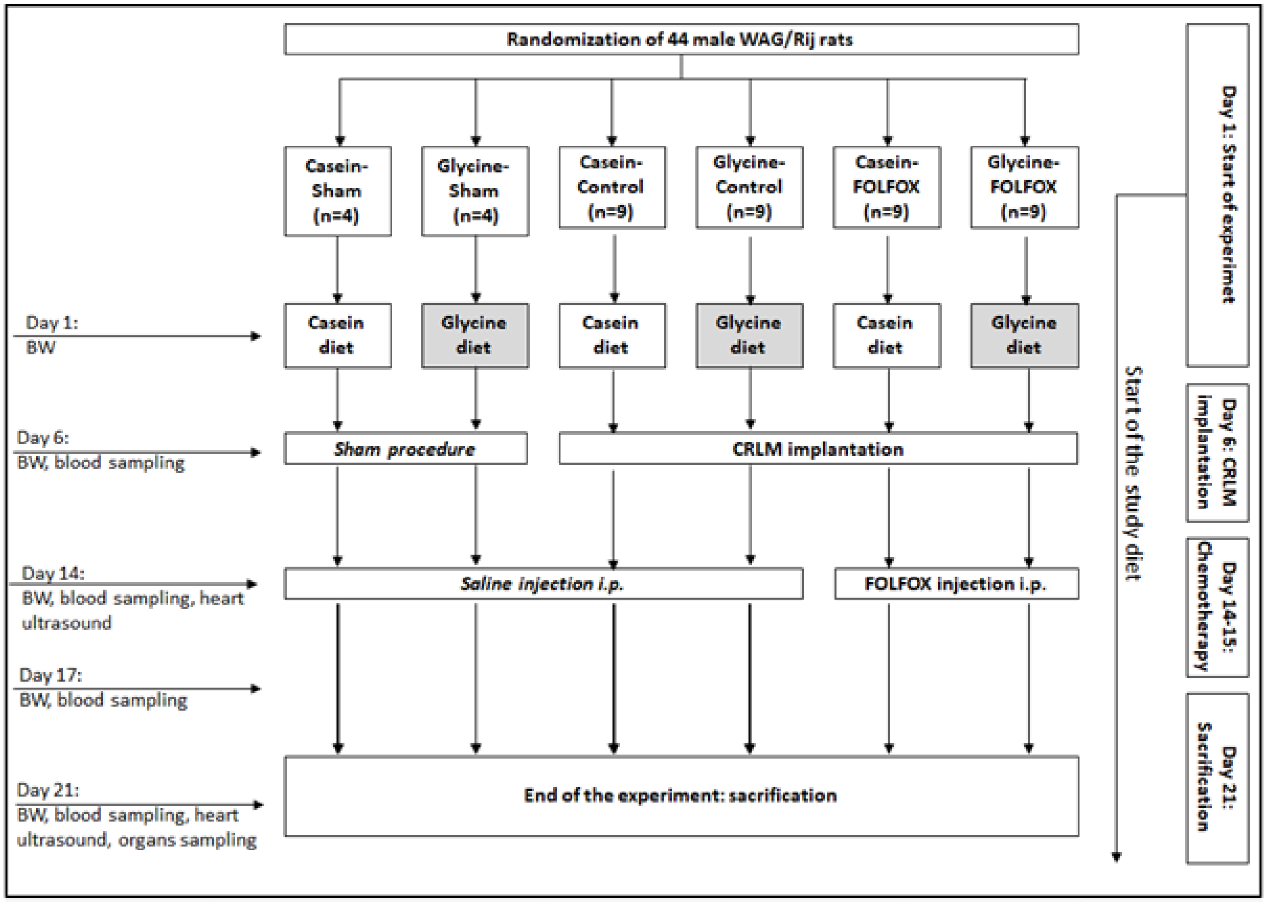

	Casein-Sham	Glycine-Sham	Casein-Control	Glycine - Control	Caseine - FOLFOX	Glycine - FOLFOX
CRLM	-	-	+	+	+	+
Glycine	-	+	-	+	-	+
FOLFOX	-	-	-	-	+	+

Figure 1. Flowchart of the animal experiment; ***adapted from*** (Maneikyte et al., 2020)***with permissions of MDPI.*** FOLFOX—chemotherapy regimen containing calcium folinate, oxaliplatin, and 5-fluorouracil; BW—body weight; CRLM—colorectal cancer liver metastasis; i.p. —intraperitoneally; ɥCT- micro-computed tomography.

2.2.3. CRLM implantation procedure

For CRLM implantation general anesthesia was induced by intramuscular injection of fentanyl (5 µg/kg) and maintained by isoflurane (2%, 2 l/min) inhalation. To prevent a decrease in body temperature through the procedure automatically regulated heating pad was always used.

Experimental rats were placed in a supine position, the right subcostal area was shaved, and a horizontal incision was made. After, 100 µl of cell suspension ($5x10^6$ CC531 cells) in PBS has been inoculated in the right liver lobe exactly under the liver capsule. The success of inoculation was verified visually. Careful hemostasis was performed, and the abdomen was closed using two layers of single-node Vicryl 4-0 (Ethicon, Somerville, NJ, USA) sutures. The skin glue (Mayer-Haake, Ober-Mörlen, Germany) was applied. The postoperative pain management protocol consisted of a single dose of carprofen (4mg/kg) applied subcutaneously and supplementing drinking water with ibuprofen (0.4 mg/ml) for the next 4-5 days (Maneikyte et al., 2019).

2.2.4. Blood sample analysis

For blood sampling on days 6, 14, 17, and 21 isoflurane anesthesia was induced, and the subclavian vein was punctured. V-Sight hematology analyzer (A. Menarini Pharma GmbH, Vienna, Austria) was used to measure complete blood count (CBC). Plasma glycine concentration on day 21 was measured in a standard hospital laboratory (Maneikyte et al., 2020). Heart fatty acid-binding protein (h-FABP) and brain natriuretic peptide (BNP) levels in plasma/serum was measured using a commercially available enzyme-linked immunosorbent assay (ELISA) kits (h-FABP; Cusabio Biotech, Newark, USA and BNP (Abcam, Cambridge, United Kingdom)) in samples obtained at the last day of the experiment. ELISAs were performed according to instructions provided by the manufacturer (Maneikyte et al., 2020).

2.2.5. µCT examination

To evaluate tumor volume experimental animals underwent µCT scans (Siemens Inveon MultiModality, Knoxville, TN, USA) on days 7 and 14 under isoflurane (2%, 2 l/min) anesthesia. To improve visualization of the liver and tumor 700 µl of commercially available contrast agent (ExiTron nano 12000; ViscoverTM, nanoPET Pharma GmbH, Berlin, Germany) was applied intravenously 24 hours before the first scan. The scanning parameters were set according to standard protocols:

- A voltage of 55 kV and a current of 500 μA;
- Exposure time of 600 ms per projection image;
- Full 360° rotation with 360 projection steps;
- Binning of 2x2 and a field of view 64 mm × 64 mm (2-bed positions);

Variable magnification settings of the scanner were set to a low level to reach an effective pixel size of 52 μm (Maneikyte et al., 2019).

2.2.6. μCT image analysis

For μCT image data analysis we used Mimics research v.20 software (Materialise, Leuven, Belgium). A specific mask (values between -602 to -247 Hounsfield Units (HU)) was created and used for the region of interest (ROI). Liver and non-liver tissue were separated with mask-splitting function. Subsequently, a 3D liver model was constructed and the organ volume was calculated. Afterward, another specific mask (values between -696 and -574 HU) was created for a tumor area. Nontumor tissue was eliminated by mask splitting function and a tumor 3D model was constructed. Tumor volume was evaluated by two independent examiners (Maneikyte et al., 2019).

2.2.7. Heart Ultrasound

Heart ultrasound using the VisualSonics Vevo 770® High-Resolution Imaging System (VisualSonics Inc., Toronto, Canada) was performed on days 7 and 14 under inhalational isoflurane (2%, 2 L/min) anesthesia. Internal diameters of the left ventricle (LV) at the level of papillary muscles were measured from left parasternal short-axis views. M-mode pictures were used to measure the left ventricular end-diastolic diameter (LVEDD) and left ventricular end-systolic diameter (LVESD) (Maneikyte et al., 2020). The ejection fraction was calculated by the Teichholz formula: $LVEF=(V_d-V_s)/V_d \times 100$, where $V_d= 7/(2.4+LVEDD)\times LVEDD^3$ and $V_s= 7/(2.4+LVESD)\times LVESD^3$ as described previously (Ríha et al., 2012).

2.3. Histology and Immunohistochemistry

Various tissue samples were taken on day 21 after experimental animals were sacrificed. Standard protocols were used to prepare paraffin-embedded sections (3 µm) of healthy liver, heart, and tumor for immunohistochemistry and histology.

2.3.1. Chromotrope aniline blue staining in heart tissue

Collagen in heart tissue was stained with chromotrope aniline blue (CAB) staining. It was performed on formalin-fixed, paraffin-embedded (FFPE) heart tissue sections in a clinical pathology laboratory at the Medical University of Graz. After CAB staining slides were scanned with Apperio AT (Wetzlar, Germany) slide scanner and viewed using Aperio ImageScope ver.12.3.2.8013 (Leica Biosystems, Wetzlar, Germany) software. Five random areas of each heart were snapshotted at 100× magnification for analysis. Quantification based on the image color analysis was performed using ImageJ (U.S. National Institutes of Health, Bethesda, Maryland, USA) software. The percentage of blue color per picture was calculated to determine the fibrosis index (Maneikyte et al., 2020).

2.3.2. Anti-Caspase 3 staining in heart tissue

Immunohistochemistry was performed in heart tissue 3 µm sections from FFPE samples. The level of apoptosis was determined using an anti-caspase 3 antibody (Abcam, Cambridge, UK; dilution 1:200, rabbit polyclonal) used together with the UltraVision LP Detection System HRP Polymer (Thermo Fisher Scientific, Waltham, MA, USA) and DAB chromogen (Dako, Via Real Carpinteria, CA, USA). Thymus tissue was stained for positive control. For negative control, primary antibodies were omitted. After staining slides were scanned and viewed using similar hardware and software as described above.

For quantification of Caspase 3 staining five snapshots at 100× magnification were taken in randomly selected areas on every slide. ImageJ software (U.S. National Institutes of Health, Bethesda, Maryland, USA) with IHC and Classic Watershed plugins was used for the analysis. The ratio of positively stained nuclei to the total number of nuclei per view was defined as the apoptotic index (Maneikyte et al., 2020).

2.3.3. Anti-Ki67 staining in tumor tissue

Healthy liver and tumor 3µm FFPE sections were prepared for immunohistochemistry according to standard protocols. The proliferation marker Ki67 (Ma et al., 2017) was used to investigate the tumor proliferation index. Anti-Ki67 antibody (Thermo Fisher Scientific, Waltham, MA, USA; dilution 1:200, rabbit IgG Clone SP6) together with the UltraVision LP Detection System HRP Polymer (Thermo Fisher Scientific, Waltham, MA, USA) and DAB chromogen (Dako, Via Real Carpinteria, CA, USA) was used. For positive control rat intestinal tissue was stained. For negative control, primary antibodies were omitted (Maneikyte et al., 2020). Previously described hardware and software were used for scanning and viewing slides.

In total 5 (3 peripheral and 2 central) tumor areas were randomly selected from each slide and snapshotted at 100x magnification for quantification of Ki67 staining. ImageJ software (U. S. National Institutes of Health, Bethesda, Maryland, USA) using IHC and classic watershed plugins were used for analysis. The ratio of stained nuclei to the total number of nuclei per view was defined as the proliferation index (Maneikyte et al., 2019).

2.3.4. Anti-CD31 staining in tumor tissue

Endothelial cells were stained with a CD31 marker to evaluate tumor microvascular density (MVD) (Lazaris et al., 2018). The anti-CD31 antibody (Abcam, Cambridge, UK; dilution 1:2000) together with the rabbit on rodent HRP-Polymer Detection System (Biocare Medical, CA, USA) and DAB chromogen (Dako, Via Real Carpinteria, CA, USA) was used. Staining was performed exactly according to the manufacturer's instructions.

Counterstaining with hematoxylin was used for both - anti-Ki67 and anti-CD31 staining procedures. For positive control rat heart tissue was stained. For negative control, primary antibodies were omitted. Previously described hardware and software were used for scanning and viewing slides.

In total 5 (3 peripheral and 2 central) tumor areas were randomly selected from each slide and snapshotted at 100x magnification for CD31 staining quantification. ImageJ (U. S. National Institutes of Health, Bethesda, Maryland, USA) software was used for analysis. The single endothelial cell positive for CD31 or clusters of them were assumed as a microvessel. MVD in different treatment groups was compared (Maneikyte et al., 2019).

2.4. Electron Microscopy

For electron microscopy, heart tissue was prepared according to this protocol:

- Fixation in 2.5% (wt/vol) glutaraldehyde and 2% (wt/vol) paraformaldehyde in 0.1 mol/L phosphate buffer, pH 7.4, for 2 h;
- Postfixation in 1% (wt/vol) osmium tetroxide for 2 h at room temperature;
- Dehydration in graded series of ethanol;
- Tissue infiltration (ethanol and agar 100 epoxy resin, pure agar 100 epoxy resin) and placement in agar 100 epoxy resin for 8 h;
- Transferring into embedding molds, and polymerization for 48 h at 60 °C;

After samples were prepared ultrathin sections (70 nm) were made using UC 7 Ultramicrotome (Leica Microsystems, Vienna, Austria). These were stained with lead citrate for 5 minutes and platin blue for 15 minutes. Tecnai G2 20 transmission electron microscope (FEI, Eindhoven, Netherlands) with a Gatan UltraScan 1000 charge-coupled device (CCD) camera at −20 °C (acquisition software Digital Micrograph; Gatan, Munich, Germany) was used to take images. The acceleration voltage was 120 kV (Maneikyte et al., 2020).

2.5. Quantitative Polymerase Chain Reaction

2.5.1. RNA Isolation and Reverse Transcription

For nucleic acid extraction samples of heart tissue were snap-frozen and stored in liquid nitrogen until the experiments. RNA isolation started by homogenizing 50–100 mg of tissue in 1 mL TRIzol reagent (Thermo Fisher Scientific, Vienna, Austria) together with a MagNA Lyser (Roche Diagnostics GmbH, Mannheim, Germany). Protocols provided by the manufacturer were used for RNA isolation. Quality and quantity were evaluated with Nanodrop 2000 (Thermo Fisher Scientific, Waltham, MA USA). For reverse transcription (High-Capacity cDNA RT Kit; Thermo Fisher Scientific, Waltham, MA USA) 2 µg of RNA was used in a final volume of 20 µL as recommended in the manufacturer protocol (Maneikyte et al., 2020).

2.5.2. Real-Time PCR

Real-time PCR amplification and melting analysis were performed using a BioRad CFX96 TouchTM System (Bio-Rad Laboratories Ges.m.b.H., Vienna, Austria) following protocols described by our group previously (Stiegler et al., 2013). cDNA corresponding to an equivalent of 5 ng RNA was added to a reaction mix containing Promega GoTaq® qPCR Master Mix (Promega, Madison Wisconsin, USA) containing 1 µM of each primer in a final reaction volume of 10 µL. The PCR reaction mixture was subjected to an initial denaturation at 95 °C for 10 seconds, followed by 45 cycles of denaturation at 95 °C for 10 seconds, annealing at 58 °C for 20 seconds, and elongation at 72 °C for 30 seconds followed by a melting curve (60 to 95 °C) (Maneikyte et al., 2020). Table 1 shows detailed information on the primers that were used.

Bio-Rad CFX Manager 3.1 (Bio-Rad Laboratories Ges.m.b.H., Vienna, Austria) with the Cq regression method embedded in the program was used to determine gene expression. All RT-PCR reactions were performed in duplicates. The housekeeping gene (ACTB) was used for data normalization. Fold change was calculated as the ratio of the target gene expression in the experimental groups (Maneikyte et al., 2020).

Table 1. Genes used for quantification and primer information; reproduced from (Maneikyte et al., 2020) ***with permission of MDPI.***

Account Number	Forward (5'->3')	Reverse (5'->3')	Product Length
COL1A1 (Collagen 1)			
NM_053304.1	CAACCTCAAGAAGTCCCTGC	AGGTGAATCGACTGTTGCCT	77bp
COL2A1 (Collagen 2)			
NM_012929.1	CAGTCGCTGGTGCTGCT	GCCCTAATTTTCGGGCATCC	76bp
BNP (Brain natriuretic peptide)			
NM_031545.1	TTTCCTTAATCTGTCGCCGCT	GGATTGTTCTGGAGACTGGCT	73bp
ACTB (beta-Actin)			
NM_031144.3	GCAGGAGTACGATGAGTCCG	ACGCAGCTCAGTAACAGTCC	74bp

2.6. Statistical Analysis

Statistical analysis was performed with SPSS v.20.0 (SPSS Inc., Chicago, Illinois, USA) software. Data are presented as median with first (Q1) and third (Q3) quartiles unless stated differently. Non-parametric tests, i.e., Mann–Whitney U test or Kruskal–Wallis test were used to analyze statistical differences between groups. Wilcoxon-Signed rank test was used for related sample analysis. Continuous data correlation was tested with a two-tailed Spearman test. All statistical tests were two-sided and p-values <0.05 were considered statistically significant.

3. Results

3.1. Cell experiments

3.1.1. Glycine effect on CC531 and HCM cells

Glycine did not affect CC531 (Fig. 2A) and HCM (Fig. 2D) cell viability at any concentration that was tested. Both chemotherapy drugs, 5-FU (Fig. 2B) and OX (Fig. 2C) had a cytotoxic effect on CC531 cells. Glycine had no additional cytotoxic effect on cell viability when combined with cytotoxic 5-FU (Fig. 2B) or OX (Fig. 2C).

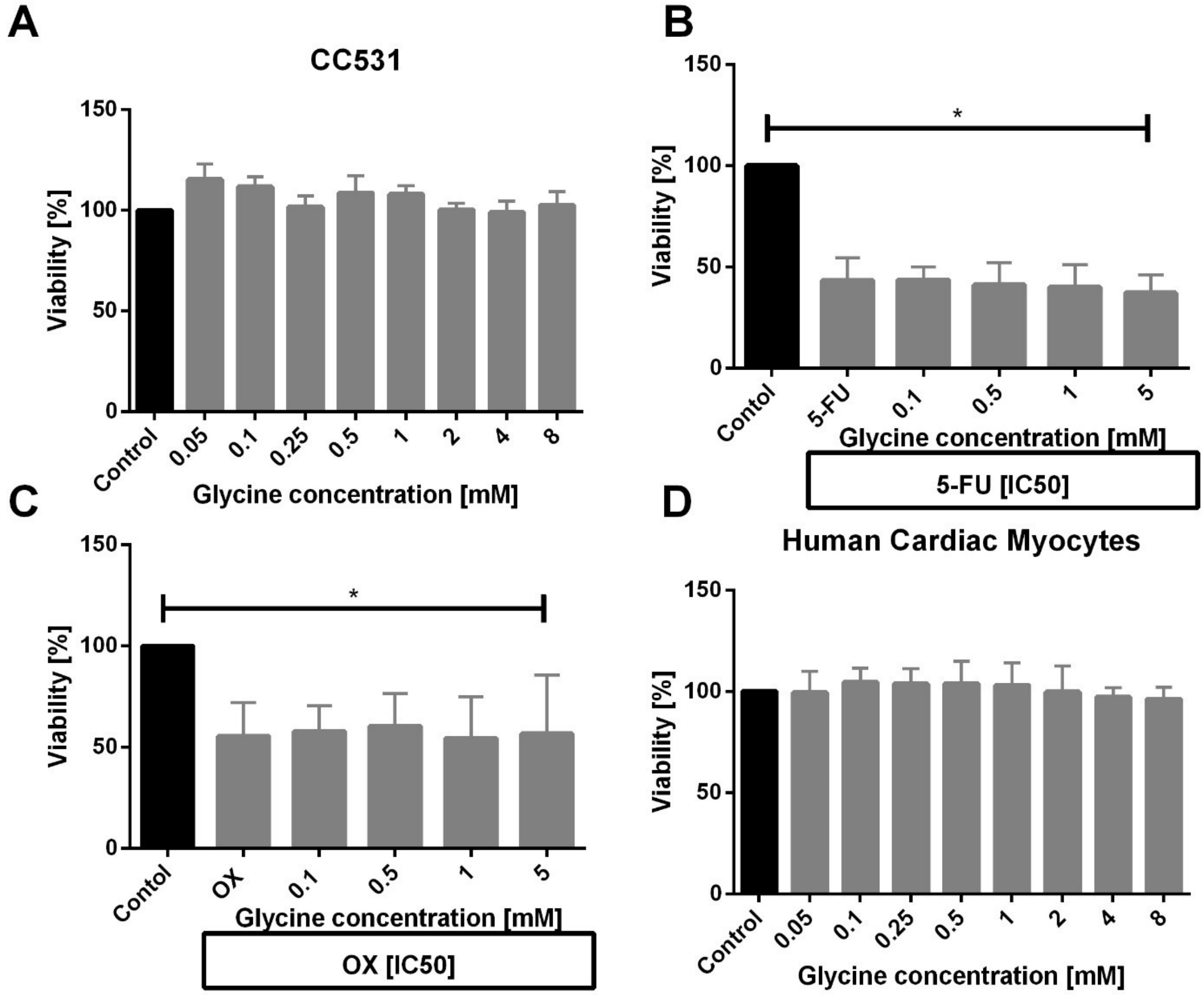

Figure 2. ***Cell viability in vitro; adapted from*** (Maneikyte et al., 2020, 2019) ***with permissions of MDPI and IVYSPRING.*** (A) CC531 viability in vitro was tested after incubation with different concentrations of glycine; (B) after incubation with 5-fluorouracil (5-FU); and (C) oxaliplatin (OX) at IC50 concentration combined with different concentrations of glycine. (D) HCM cells viability after incubation with different concentrations of glycine was measured by MTT assay and presented as the percentage of the controls. MTT assay was performed as described in the methods. Results are presented as a mean±SD. * for significance with $p<0.05$.

3.2. Animal experiments

3.2.1. General health conditions and body weight.

Most of the rats (43; 97.7%) rats underwent the full experimental protocol. Any of the study-related procedures affected experimental animals, except, FOLFOX, which caused diarrhea, decreased food intake, and resulted in weight loss. Daily food consumption drastically decreased from 12 g (9; 13.5) to less than 1 g per rat ($p<0.05$). Such impact of CTx was observed irrespective of diet type and persisted for two days followed by normalization on day 16. This temporary starvation caused weight loss in CTx-treated animals. On day 21 the median weight of rats in Glycine-FOLFOX and Casein-FOLFOX groups was 90% and 93% of baseline weight, respectively. In contrast, the weight of animals without CTx steadily increased and reached 123–129% of baseline weight, $p < 0.05$ (Figure 3) (Maneikyte et al., 2020, 2019).

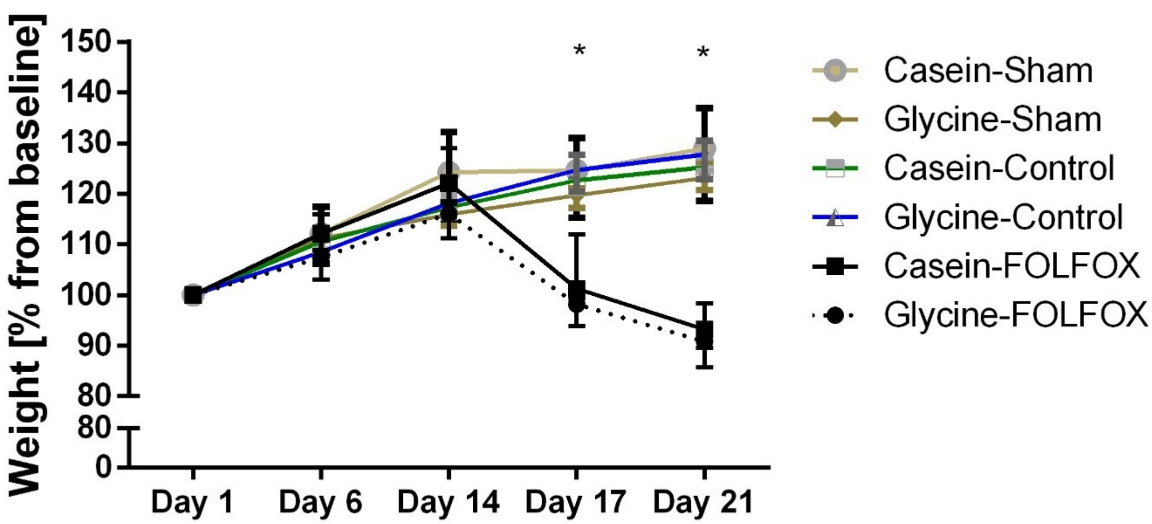

Figure 3. ***Animal body weight.*** Animal body weight was measured on days 1, 6, 14, 17, and 21. The median body weight was steadily increasing until FOLFOX was applied on day 14. The median weight of animals on days 17 and 21 in FOLFOX groups with glycine or casein was significantly lower compared to corresponding controls. Results are presented as a median and interquartile range. * for significance with $p<0.05$.

3.3. Hemoglobin and blood cell count

Experimental treatment did not affect red blood cell (RBC) and hemoglobin (HGB) levels which were stable and similar between the groups throughout the experiment. CTx significantly decreased white blood cells (WBC) and platelet (PLT) levels which resulted in severe leukopenia and thrombocytopenia. After FOLFOX application, WBC levels significantly decreased from 11.5 x 10^9/l (8.5; 12.9) before CTx to 0.5 x 10^9/l (0.37; 0.7) at the end of the study (p=0.001). Similarly, PLT levels decreased from 933 x 10^9/l (151; 1153) to 105 x 10^9/l (31; 203) (p=0.002). Diet did not prevent FOLFOX-induced leukopenia, although, it significantly diminished the decrease of PLT levels (203 (139; 238) vs 36 (23; 58), p=0.001) (Table 2) (Maneikyte et al., 2020, 2019).

Table 2. Hemoglobin, red blood cell, white blood cell, and platelets count at different time points of the study.

		Glycine-FOLFOX	Casein-FOLFOX	Glycine-Control	Casein-Control	Glycine-Sham	Casein-Sham	p-value
HGB; g/l Median (Q1; Q3)	Day 6	149 (139; 162)	149 (142; 168)	160 (140; 176)	150 (143; 170)	143 (138; 155)	153 (134; 153)	0.869
	Day 14	161 (154; 173)	167 (133; 174)	152 (148; 160)	153 (145; 174)	167 (165; 186)	158 (147; 166)	0.422
	Day 21	161 (144; 175)	159 (151; 169)	164 (154; 209)	168 (145; 171)	142 (139; 150)	146 (112; 150)	0.093

RBC x 10^{12}/l Median (Q1; Q3)	Day 6	7.68 (7.14; 8.49)	7.65 (7.29; 8.24)	7.98 (7.07; 8.67)	7.58 (7.05; 8.45)	7.69 (7.10; 8.22)	7.74 (6.99; 7.74)	0.989
	Day 14	8.10 (7.94; 8.75)	8.45 (6.97; 9.12)	7.56 (7.39; 8.21)	8.01 (7.39; 8.85)	8.55 (8.43; 9.50)	8.23 (7.70; 8.33)	0.273
	Day 21	8.81 (7.72; 9.24)	8.35 (7.69; 9.01)	8.53 (7.83; 10.29)	8.46 (7.44; 8.85)	7.53 (7.31; 7.92)	7.43 (5.64; 7.78)	0.108
PLT x10^9/l Median (Q1; Q3)	Day 6	768 (398; 1097)	457 (114; 1044)	648 (280; 858)	803 (158; 861)	526 (122; 1004)	153 (62; 153)	0.610
	Day 14	1056 (559; 1249)	174 (105; 1014)	980 (918; 1139)	761 (586; 1123)	602 (269; 1332)	196 (132; 662)	0.103
	Day 21	203 (139; 238)	36 (23; 58)	887 (445; 1075)	1021 (779; 1283)	1155 (1105; 1223)	1014 (253; 1182)	0.001
WBC x10^9/l Median (Q1; Q3)	Day 6	11.1 (9.0; 12.4)	10.4 (9.6; 11.6)	11.7 (10.6; 12.2)	11.0 (10.7; 11.9)	10.1 (9.7; 12.3)	10.7 (8; 10.7)	0.701
	Day 14	11.5 (9.5; 13.0)	11.6 (4.8; 12.7)	11.6 (10.4; 15.8)	14.8 (10.5; 17.1)	9.6 (8.7; 11.2)	10.2 (9.7; 10.4)	0.088
	Day 21	0.5 (0.3; 0.9)	0.4 (0.2; 0.6)	8.4 (7.3; 9.3)	8.9 (7.3; 9.6)	6.8 (6.1; 7.7)	7.0 (3.3; 8.4)	0.001

3.4. Blood biochemistry: total protein, albumin, blood urea nitrogen, and bilirubin

FOLFOX induced a significant decrease in total protein and albumin levels. Total protein and albumin levels in animals receiving FOLFOX decreased from 5.2 (5.0; 5.5) and 3.0 (2.8; 3.0) prior to CTx to 3.6 (3.2; 3.9; p=0.001) and 1.9 (1.6; 2.2; p=0.001) on the last day of the experiment, respectively. Diet did not affect total protein and albumin levels in rats treated with FOLFOX at any time point of the experiment (Table 3).

Table 3. Total protein, albumin, blood urea nitrogen, and bilirubin levels at different time points of the study.

		Glycine-FOLFOX	Casein-FOLFOX	Glycine-Control	Casein-Control	Glycine-Sham	Casein-Sham	p-value
Total protein; g/dl Median (Q1; Q3)	Day 6	4.9 (4.7; 5.1)	5.0 (4.6; 5.3)	4.9 (4.6; 5.2)	5.1 (4.7; 5.1)	4.9 (4.8; 5.1)	5.1 (4.8; 5.5)	0.862
	Day 14	5.1 (5.0; 5.4)	5.4 (5.0; 5.5)	5.1 (5.0; 5.3)	5.2 (4.9; 5.3)	5.3 (4.9; 5.7)	5.0 (4.7; 5.4)	0.492
	Day 21	3.9 (3.5; 4.0)	3.2 (3.1; 3.7)	4.6 (4.2; 4.8)	5.1 (4.7; 5.3)	4.7 (4.7; 4.9)	5.0 (4.7; 5.4)	0.001
Albumin; g/dl Median (Q1; Q3)	Day 6	2.9 (2.7; 3.0)	3.0 (2.8; 3.1)	2.9 (2.7; 3.0)	3.1 (2.9; 3.1)	2.8 (2.7; 2.9)	3.1 (3.0; 3.2)	0.065

	Day 14	3.0 (2.9; 3.0)	3.0 (2.7; 3.1)	2.8 (2.8; 3.0)	2.9 (2.8; 3.0)	3.0 (2.9; 3.3)	2.9 (2.6; 3.0)	0.724
	Day 21	2.2 (1.9; 2.4)	1.7 (1.5; 1.9)	2.5 (2.5; 2.7)	2.9 (2.8; 3.0)	2.9 (2.8; 3.1)	3.0 (2.8; 3.1)	0.001
Total bilirubin; mg/dl Median (Q1; Q3)	Day 6	0.4 (0.2; 0.4)	0.3 (0.2; 0.8)	0.4 (0.3; 0.4)	0.3 (0.3; 0.4)	0.2 (0.2; 0.4)	0.4 (0.4; 0.4)	0.743
	Day 14	0.4 (0.3; 0.4)	0.3 (0.3; 0.4)	0.3 (0.3; 0.4)	0.4 (0.3; 0.5)	0.6 (0.4; 0.7)	0.3 (0.3; 0.4)	0.142
	Day 21	0.3 (0.3; 0.5)	0.4 (0.3; 0.5)	0.2 (0.1; 0.3)	0.2 (0.1; 0.4)	0.3 (0.2; 0.4)	0.3 (0.2; 0.3)	0.011

3.5.Blood biochemistry: Liver injury markers

FOLFOX significantly increased aspartate aminotransferase (AST) and alanine aminotransferase (ALT) levels. Following one cycle of FOLFOX application, AST levels increased 3-fold from 31 (27; 42) IU/l to 94 (58; 103) IU/l at 3 days after chemotherapy (p=0.001). Similarly, ALT levels increased from 13 (11; 15) to 32 (26; 37) (p=0.001).
Diet did not affect AST and ALT levels in rats treated with FOLFOX at any time point. ALT and AST levels remained stable in groups without FOLFOX (Figure 4).

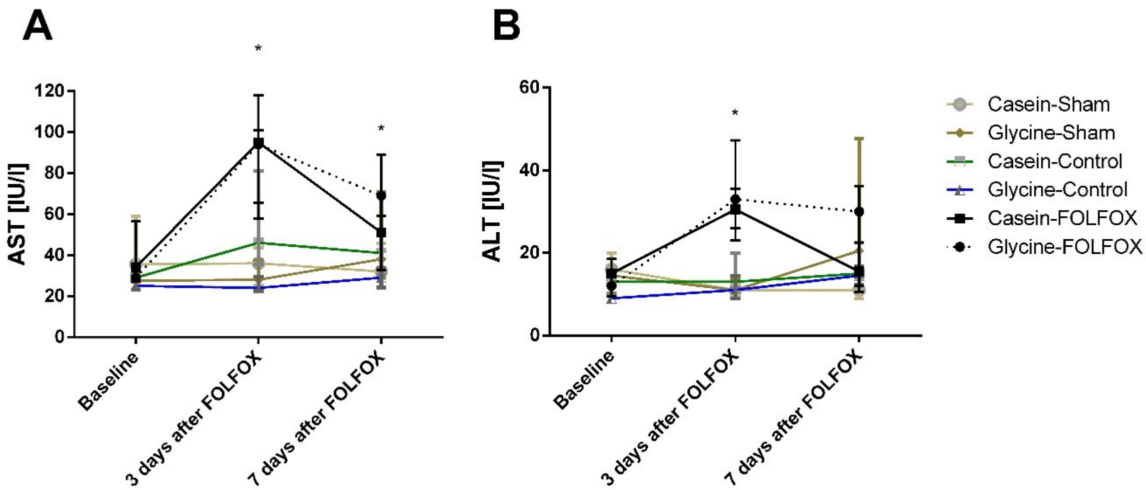

Figure 4. ***Levels of serum transaminases after FOLFOX.*** FOLFOX significantly increased AST (A) and ALT (B) levels in Glycine-FOLFOX and Casein-FOLFOX groups, irrespective of the diet type. Results are presented as a median and interquartile range. * for significance with p<0.05. AST and ALT levels in Casein-FOLFOX and Glycine-FOLFOX groups were significantly higher compared to corresponding controls at 3 days after FOLFOX.

3.6. Plasma glycine concentration

Glycine enriched diet increased plasma glycine concentration almost fivefold (955 (400; 1250) µmol/L vs. 190 (126; 285) µmol/L; p=0.001).

3.7. Liver and tumor volume.

Liver volumes in different study groups were not different as measured by µCT liver scan on day 21, p=0.170 (Figure 5). However, scans revealed significantly different CRLM tumor volumes between different treatment groups, p=0.028. Glycine alone and in combination with FOLFOX decreased CRLM growth from 292 (193; 671) mm^3 and 271 (140; 443) mm^3 to 123 (193; 671) mm^3 and 98 (19; 165) mm^3, respectively (p<0.05) (Figure 6). Furthermore, CRLM after treatment with glycine plus FOLFOX was smaller, but the differences were not significant, p=0.281 (Figure 6) (Maneikyte et al., 2019).

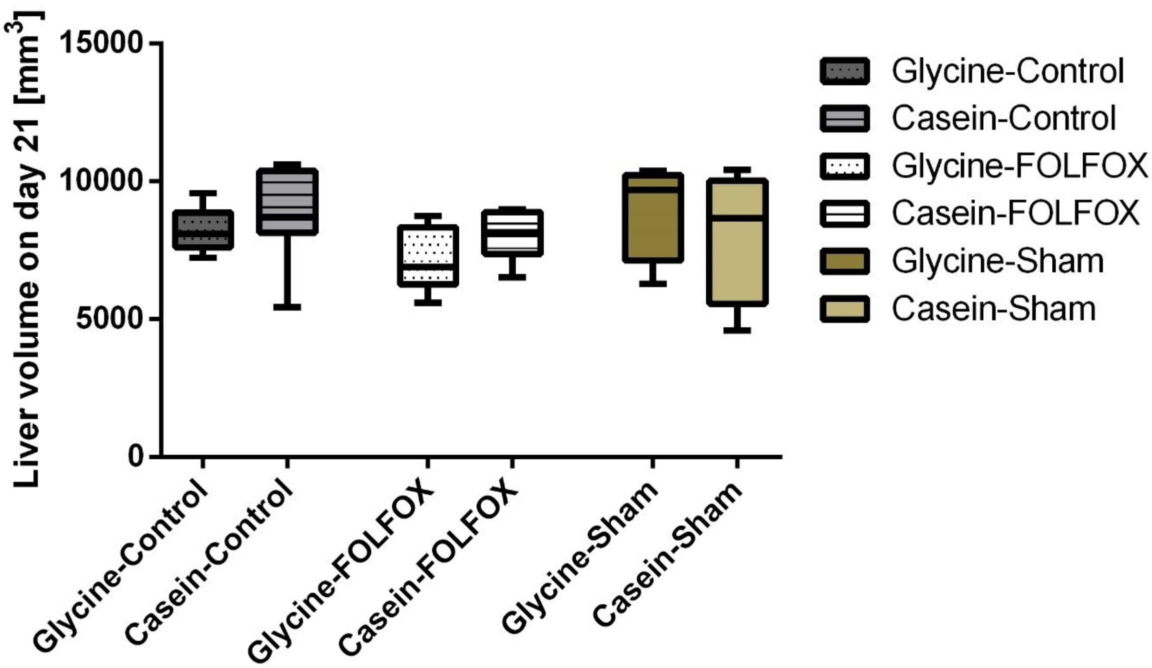

Figure 5. ***Liver volume on the last day of the experiment in different treatment groups.*** The liver volume was calculated as described in the methods.

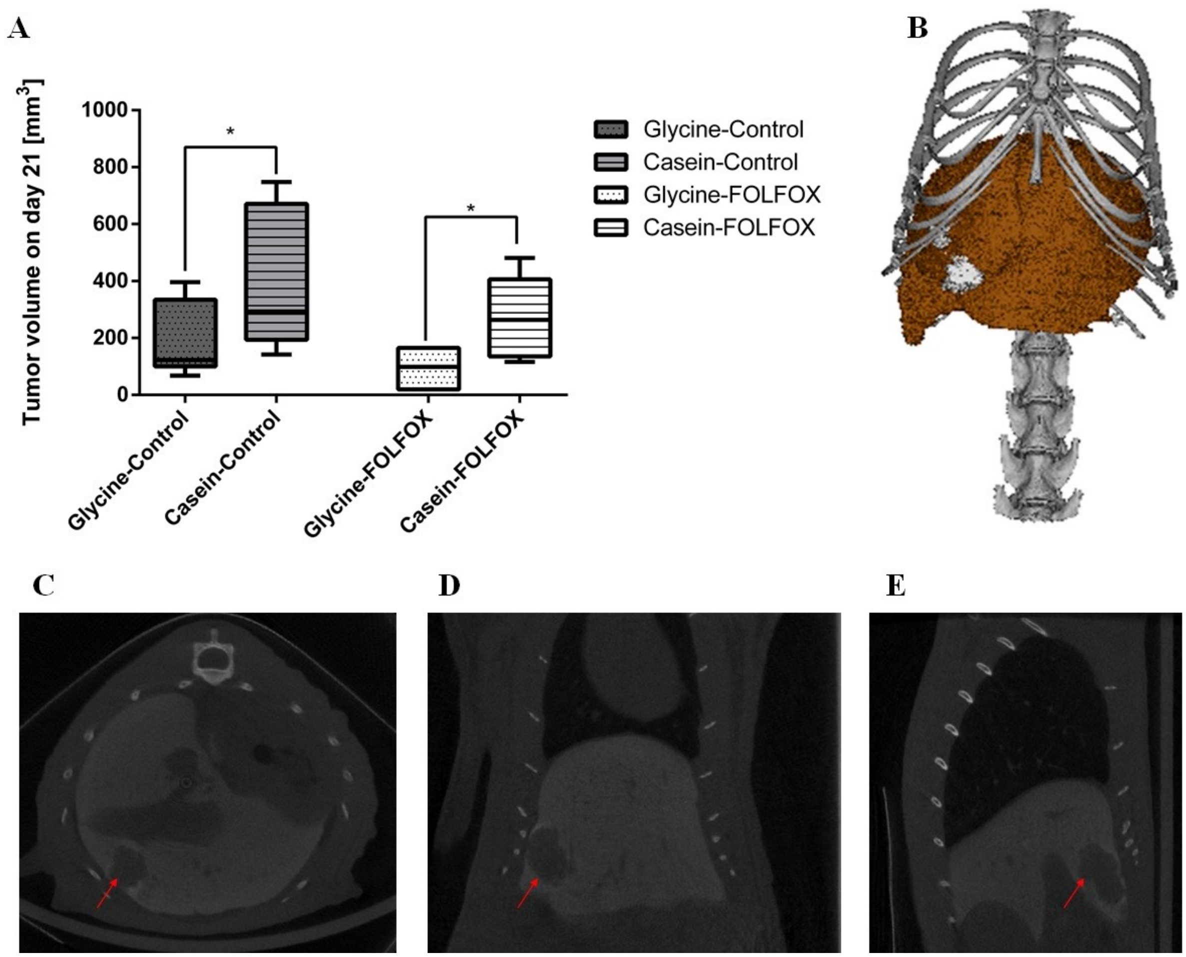

Figure 6. ***Tumor volume on the last day of the experiment in different treatment groups by μCT.*** A: Tumor volumes in different study groups. B: Representative 3D reconstruction of liver μCT scan C: Representative liver μCT scan, axial section; red arrow indicates colorectal cancer liver metastasis; D: Representative liver μCT scan, coronal section; red arrow indicates colorectal cancer liver metastasis; E: Representative liver μCT scan, sagittal section; red arrow indicates colorectal cancer liver metastasis. Tumor volume was calculated as described in the methods. *for significance with $p<0.05$.

3.8. Proliferation index

Glycine had no effect on tumor proliferation index by Ki67 staining with an index of 3.6 (0.6; 7.9) % compared to 4.0 (1.9; 7.0) % in the corresponding controls (Figure 7). Likewise, proliferation was not significantly decreased by FOLFOX as well (4.0 (1.9; 7.0) % vs 2.3 (0.8; 3.4) %, $p>0.05$). Glycine in combination with FOLFOX was most effective in decreasing tumor proliferation by 62% (0.8 (0.7; 1.8) %), however, the difference was not significant (Figure 7) (Maneikyte et al., 2019).

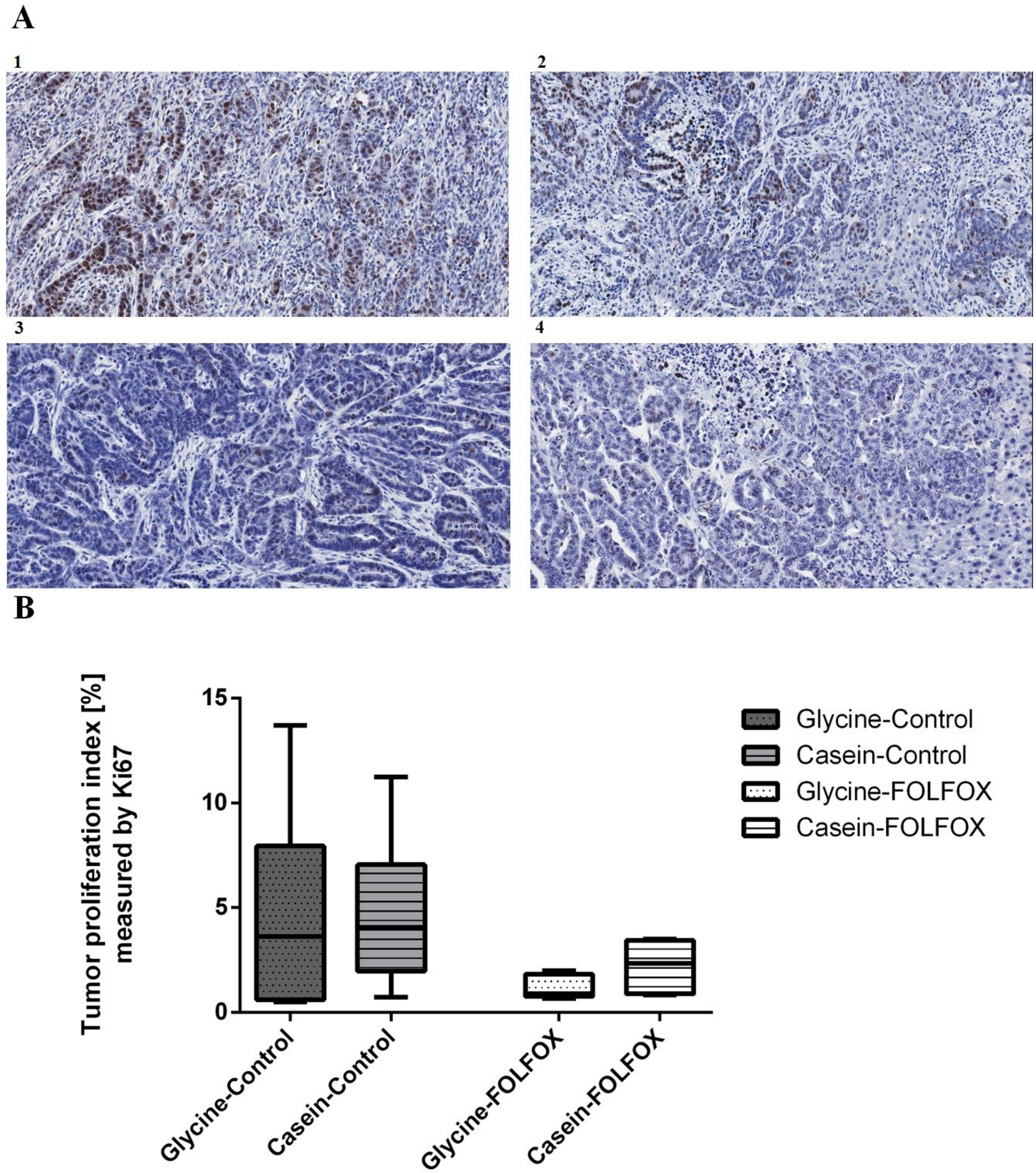

Figure 7. ***Tumor proliferation index by Ki67 staining in study groups; adapted from Maneikyte et al. 2019 with permissions of IVYSPRING.*** A: Representative pictures of tumors stained with

anti-Ki67 antibody in (1) Casein-Control, (2) Glycine-Control, (3) Casein-FOLFOX, and (4) Glycine-FOLFOX. B; comparison of proliferation index between the groups. Both groups treated with FOLFOX showed a tendency ($p<0.1$) to have a lower tumor proliferation index, however, the differences were not significant.

3.9. Tumor vascularization

Tumor MVD was significantly different among the study groups, $p=0.004$. Glycine alone and in combination with FOLFOX decreased MVD from 57 (48; 81) to 16 (14; 29), $p=0.003$, and from 46 (39; 83) to 9 (9; 46) MVD per field, $p=0.048$, respectively. In contrast, FOLFOX alone did not affect MVD (Figure 8) (Maneikyte et al., 2019).

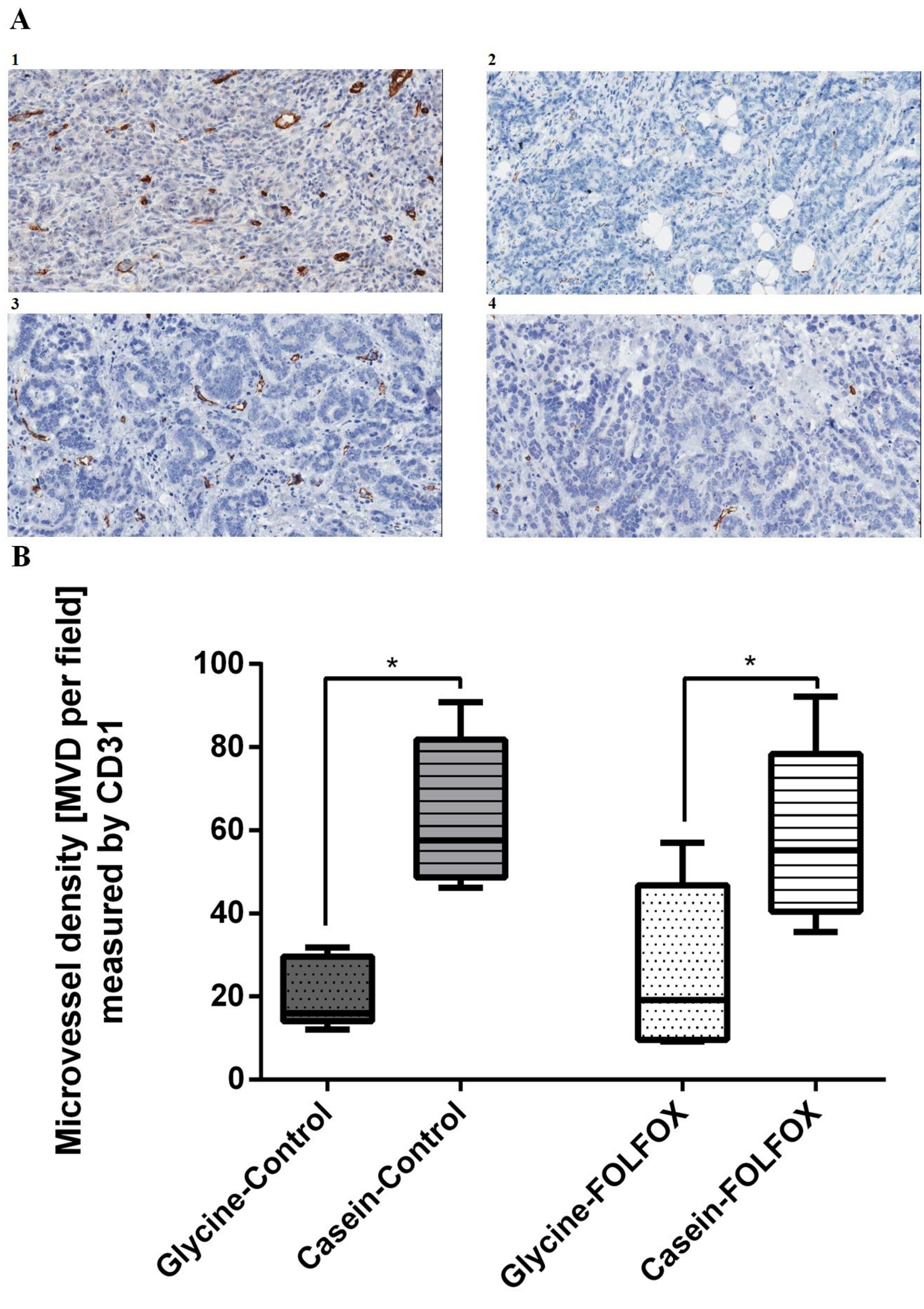
A
1
2
3
4
B
Microvessel density [MVD per field] measured by CD31
100
80
60
40
20
0
*
*
Glycine-Control
Casein-Control
Glycine-FOLFOX
Casein-FOLFOX

Figure 8. ***Tumor microvascular density (MVD) in different treatment groups; adapted from Maneikyte et al. 2019, with permissions of IVYSPRING.*** A: representative pictures of tumors stained with anti-CD31 antibody in (1) Casein-Control, (2) Glycine-Control, (3) Casein-FOLFOX, and (4) Glycine-FOLFOX. B: comparison of MVD between groups. Glycine significantly reduced the MVD irrespective of FOLFOX; * for significance with p<0.05.

3.10. h-FABP Concentrations in Serum

Treatment with FOLFOX increased the h-FABP level to 1760 (941; 5000) pg/mL compared to 728 (386; 900) pg/mL and 158 (86; 267) in controls, p=0.001. Glycine diminished such increase by 35%, although the difference failed for significance (1904 (1265; 5514) vs 1240 (698; 4929) pg/mL, p=0.195 (Figure 9) (Maneikyte et al., 2020).

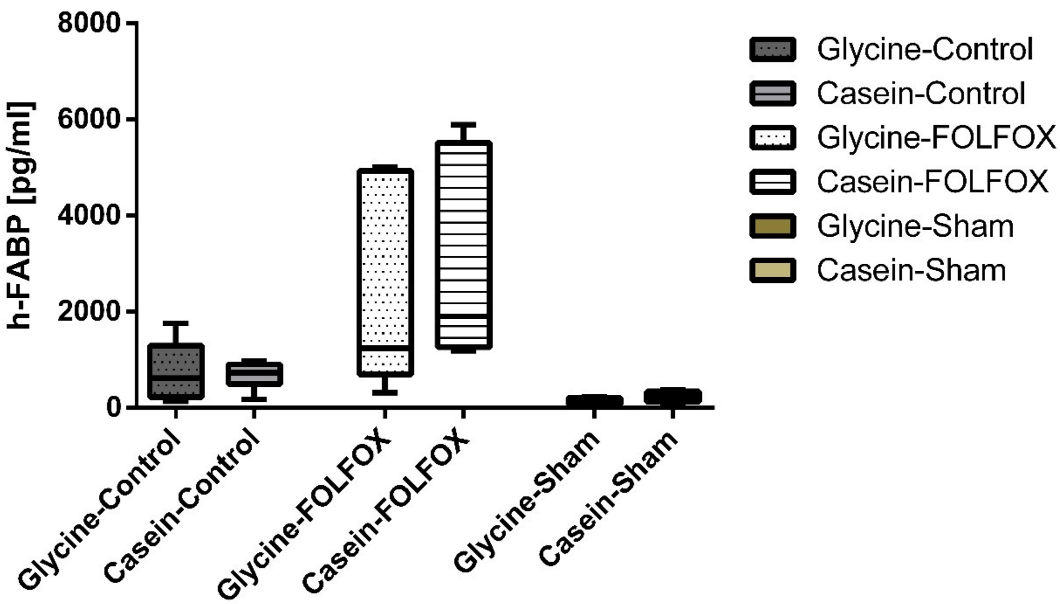

Figure 9. ***Serum levels of h-FABP on the last experimental day; adapted from Maneikyte et al. 2020, with permissions of MDPI.*** The h-FABP level measured on the last experimental day was different between the study groups. *=p<0.05. Groups that received chemotherapy (Casein-FOLFOX, Glycine-FOLFOX) had a significantly higher h-FABP level compared to groups that had not received chemotherapy (Glycine-Control; Casein-Control; Glycine-Sham; Casein-Sham). Although, the difference between Casein-FOLFOX and Glycine-FOLFOX groups was not significant.

3.11. Left Ventricle Ejection Fraction

Before CTx LVEF was similar across the study groups and ranged from 76% to 82%, p = 0.207. Treatment with FOLFOX significantly decreased LVEF from 82% (78; 85) to 72% (65; 81), p = 0.028. In contrast, dietary glycine prevented this decrease. CRLM alone did not affect LVEF. (Figure 10).

The FOLFOX-induced decline of LVEF significantly correlated with the myocardial fibrosis index (R = 0.731, p = 0.005) and the serum h-FABP level (R = 0.572, p = 0.033). The apoptotic index of the heart muscle, as well as BNP, type I, and II collagen gene expression levels, did not correlate with the decrease of LVEF (Maneikyte et al., 2020).

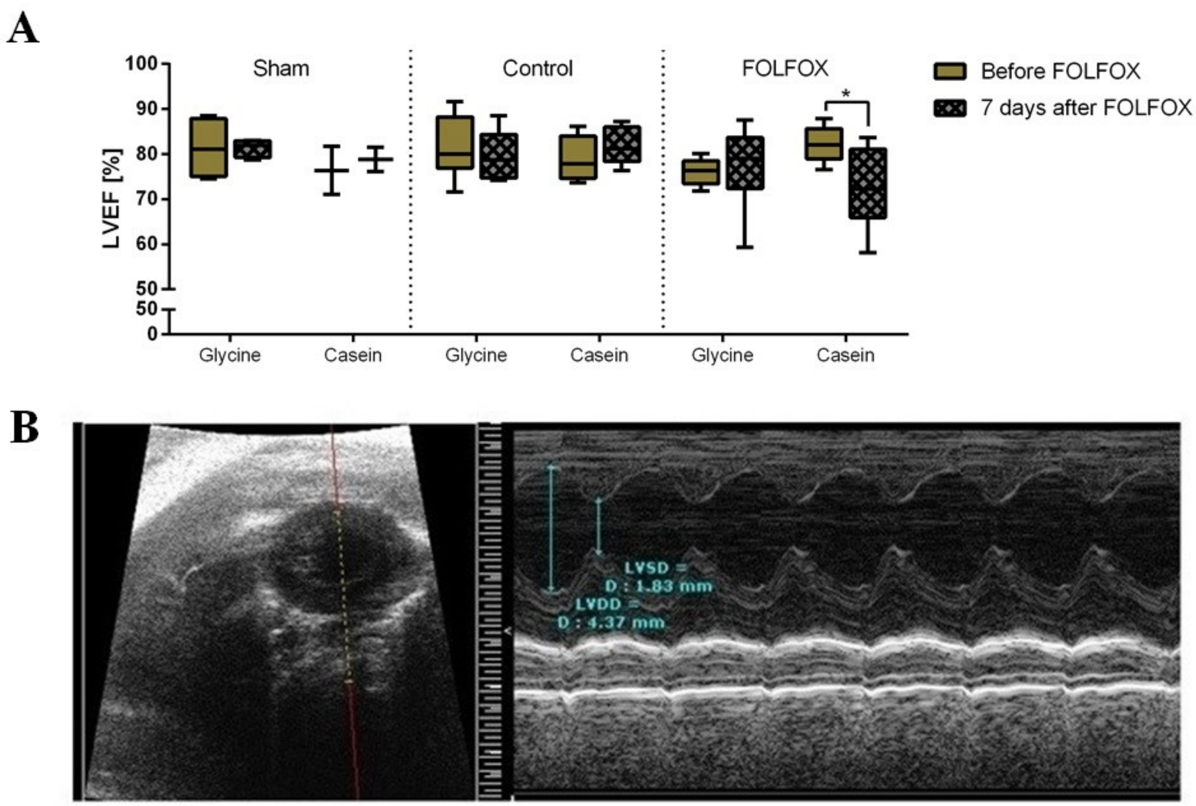

Figure 10. ***Left ventricle ejection fraction (LVEF) before and after FOLFOX chemotherapy in different diet groups; adapted from Maneikyte et al. 2020, with permissions of MDPI.*** (A) Left ventricle ejection fraction (LVEF) before and after chemotherapy or sham treatment in the study groups; * $p < 0.05$. (B) Representative view from heart ultrasound. Left: Heart in parasternal short-axis view; Right: M-mode, left ventricular internal diameters.

3.12. Fibrosis Index in the Myocardium by CAB staining

FOLFOX increased myocardial fibrosis. The highest fibrosis index, as measured by CAB staining, of 5.1% (4.5; 7.0 %) was seen in the Casein-FOLFOX group. Dietary glycine precluded such CTx-induced increase in fibrosis. Compared to the Casein-FOLFOX group the fibrosis index in the Glycine-FOLFOX group was lower by 33% (3.4 (3.1; 4.3), p=0.012. Moreover, the fibrosis index in the Glycine–FOLFOX group was not significantly different compared to the groups that did not receive FOLFOX (Figure 11).

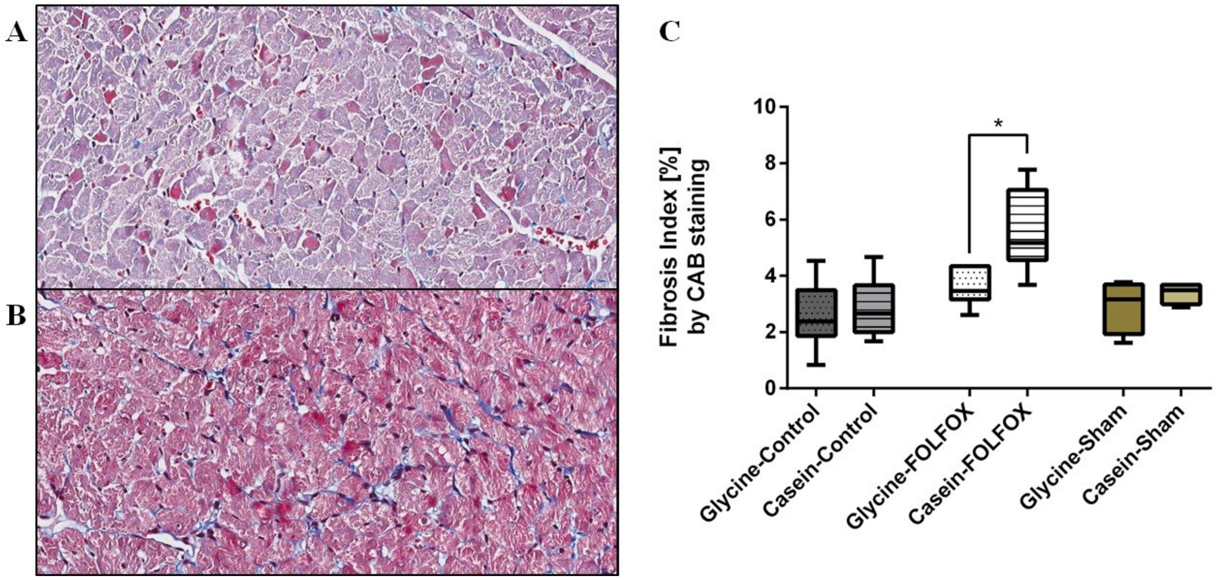

Figure 11. Fibrosis index measured by chromotrope aniline blue staining; adapted from Maneikyte et al. 2020, with permissions of MDPI. Representative pictures at 100× magnification of CAB stain for fibrous tissue in the myocardium of animals treated with FOLFOX and glycine (A) or FOLFOX and casein (B). The amount of fibrosis between the study groups was different (C). * Glycine significantly reduced fibrosis index in the groups treated with FOLFOX, $p < 0.05$.

3.13. Apoptotic Index in the Myocardium

FOLFOX increased apoptosis level in the heart tissue. The highest proportion of caspase 3 positive cells was in Casein–FOLFOX group (11.0 (5.8; 18.1) %). Dietary glycine reduced FOLFOX-induced apoptosis. The apoptotic index was reduced by 3.5-fold to 3.0 (1.3; 6.3) %, $p=0.015$. Apoptotic index in the Glycine–FOLFOX group was similar to that in groups that did not receive FOLFOX, $p>0.05$ (Figure 12) (Maneikyte et al., 2020).

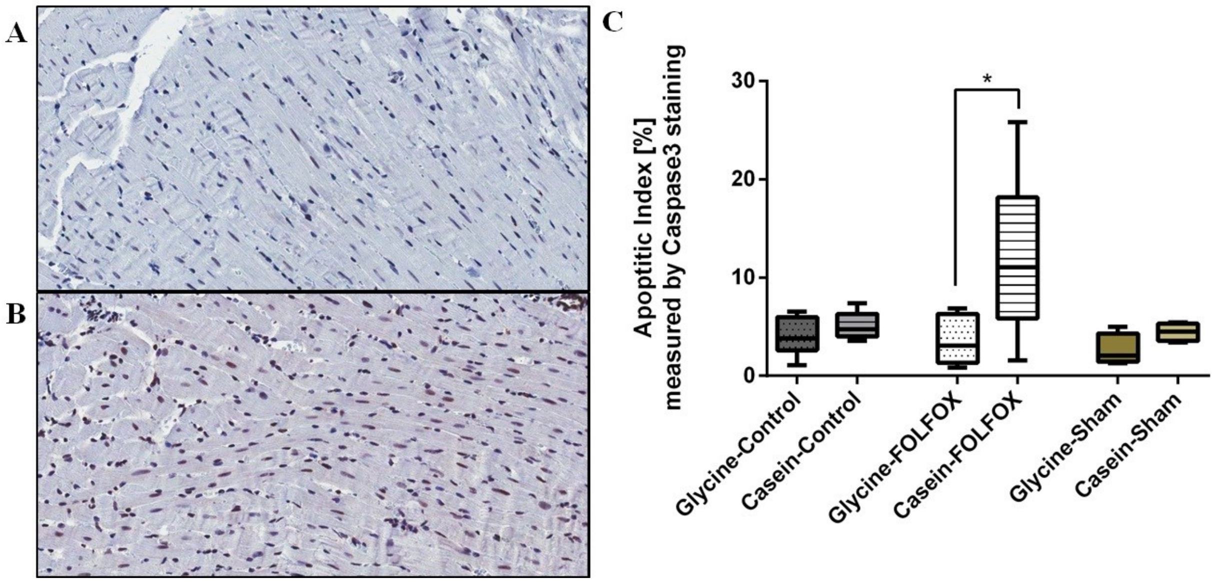

Figure 12. The apoptotic index measured by immunohistochemistry with anti-Caspase 3 antibody; adapted from Maneikyte et al. 2020, with permissions of MDPI. Representative pictures at 100× magnification of anti-Caspase 3 staining for fibrous tissue in the myocardium of animals treated with FOLFOX and glycine (A) and FOLFOX alone (B). The caspase 3 positive cells rate was significantly higher in the Casein-FOLFOX group compared to the Glycine-FOLFOX group, * $p < 0.05$ (C).

3.14. Electron Microscopy of Heart Tissue

Figure 13 shows representative images of transmission electron microscopy from different treatment groups. Normal heart architecture was seen in groups that did not receive FOLFOX (Casein–Sham, Glycine–Sham, Casein–Control, and Glycine–Control) (Figure 13A). Changes in the heart tissue including collagen fibers within the heart muscle and lysosomes within the endothelial cells have been observed after treatment with FOLFOX in the Casein-FOLFOX group (Figure 13B). Although, these changes were absent in the rats who received FOLFOX but together with glycine diet (Figure 13C) (Maneikyte et al., 2020).

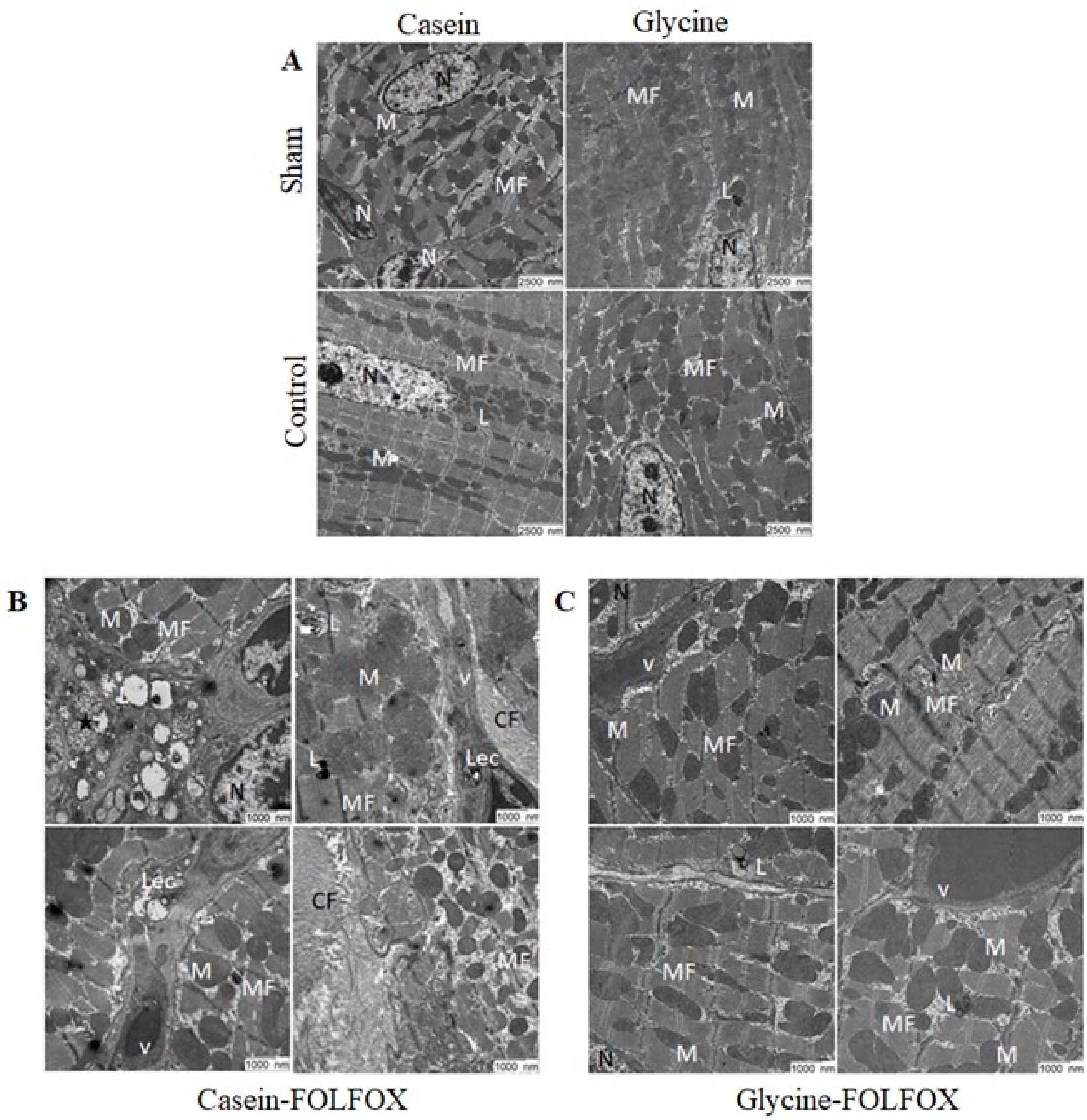

Figure 13. Transmission electron microscopy scans of heart samples; reproduced from Maneikyte et al. 2020, with permissions of MDPI. Representative pictures of hearts scanned by electron microscopy in (A) groups without FOLFOX (Casein–Sham, Glycine–Sham, Casein–Control, Glycine–Control) at magnification 7000×; (B) Casein–FOLFOX; and (C) Glycine–FOLFOX groups at magnification 12,000×. FOLFOX induced a significant increase in collagen fibers in the heart muscle and lysosomes within the endothelial cells in the Casein–FOLFOX group. Glycine prevented FOLFOX-induced ultrastructural changes. MF—myofibrils; M—

mitochondria; N—nucleus, L—lysosomes; Lec—lysosomes within endothelial cells; asterisk—lysosomes containing dark granules and other lipids; v—vessels; CF—collagen fibers.

3.15. Brain natriuretic peptide, Collagen I, and Collagen II gene expression in heart tissue

FOLFOX induced the upregulation of type I collagen gene expression compared to that in corresponding controls, $p < 0.05$. However, there were no differences between Casein–FOLFOX and Glycine–FOLFOX groups, p=0.999 (Figure 14A). Expression of type II collagen (Figure 14B) and BNP (Figure 14C) genes was similar across all the study groups (Maneikyte et al., 2020).

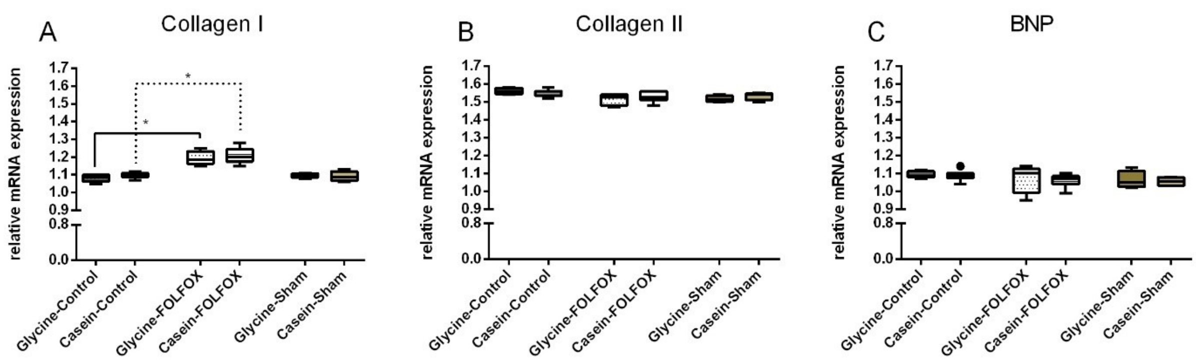

Figure 14. Type I and II collagen and brain natriuretic peptide (BNP) gene expression in the heart muscle; ***reproduced from Maneikyte et al. 2020, with permissions of MDPI.*** Type I collagen gene expression was significantly increased in FOLFOX groups (Casein–FOLFOX; Glycine–FOLFOX) compared to that in corresponding controls (Casein–Control; Glycine–Control), * $p < 0.05$. There was no difference between Casein–FOLFOX and Glycine–FOLFOX groups (A). Type II collagen (B) and BNP (C) expression were not different between the study groups.

3.16. Total cholesterol and high-density lipoprotein concentrations in serum

FOLFOX significantly increased total cholesterol level to 64 (58; 67) mg/dL compared to 49 (49; 53) mg/dL in controls, p=0.001, and 49 (49; 49) mg/dL in sham groups, p=0.001. The type of diet had no impact on total cholesterol and HDL levels (Figure 15).

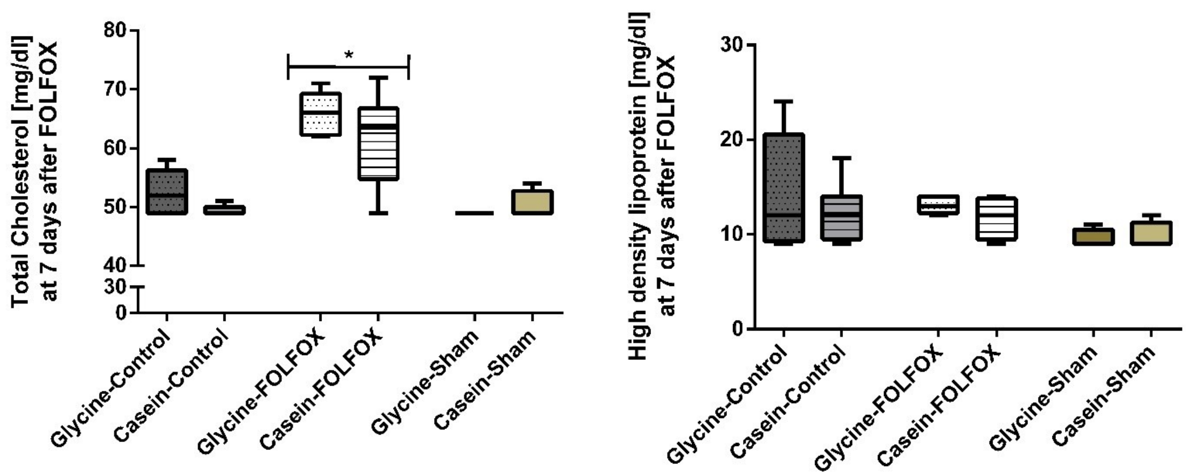

Figure 15. ***Serum levels of total cholesterol and high-density lipoprotein on the last experimental day.*** FOLFOX increased total cholesterol level. Glycine had no impact on total cholesterol and HDL levels. *=p<0.05.

4. Discussion

This experimental study investigated the anti-tumorigenic and cardioprotective potential of dietary glycine in an experimental in vivo model of CRLM treatment with conventional FOLFOX CTx. The results presented here showed that glycine can reduce the growth of CRLM. Moreover, it has a significant cardioprotective effect against FOLFOX-induced reduction of LVEF by reducing fibrosis and apoptosis level in myocardial tissue.

Previously the antitumorigenic properties of glycine have been suggested by Rose et al. (Rose et al., 1999b, 1999a). These previous studies showed inhibition at a greater extent of larger tumors than smaller tumors by glycine in carcinogen (WY-14,643) induced liver cancer (Rose et al., 1999a). Thus glycine was hypothesized to have anti-angiogenic properties, which prevent tumor growth by inhibiting tumor neovascularization (Maneikyte et al., 2019; Rose et al., 1999a). Further, this hypothesis was supported in a subsequent experimental study where glycine was shown to inhibit melanoma tumor vascularization in mice (Maneikyte et al., 2019; Rose et al., 1999b). A similar mechanism was described by Bruns et al. in a study investigating the glycine effect on HUVEC cells growth and angiogenesis (Bruns et al., 2016). The results of the study demonstrated that glycine-blunted VEGF-stimulated cells' growth, migration, and angiogenesis, but had no direct impact on the viability and proliferation of HUVEC cells (Bruns et al., 2016; Maneikyte et al., 2019). Furthermore, this study provided evidence for glycine receptors' α1 and α2 subunits expression in HUVEC cells (Bruns et al., 2016). These receptors role in angiogenesis inhibition was confirmed by showing that the glycine effect can be prevented by strychnine, which is a well-known antagonist of the glycine receptor (Nagy et al., 1989). The results of our study clearly indicate that anti-angiogenic properties of glycine are also present in vivo as it significantly reduced MVD in CRLM. Angiogenesis is critical for solid cancer growth as diffusion alone cannot supply adequate oxygen and nutrition to maintain larger-sized tumors. (Maneikyte et al., 2019; Nagy et al., 1989; Takahashi et al., 2003). Hence, highly vascularized tumors have a propensity for growth and subsequently result in poorer patient outcomes. Specifically, high MVD by anti-CD31 staining in CRC tumors is conversely related to patients' survival (Guetz et al., 2006). Therefore, it can be interpreted that glycine inhibits CRLM growth by decreasing the microvascularization of the tumor (Maneikyte et al., 2019).

To the contrary, some authors report the pro-tumorigenic effects of glycine (Maneikyte et al., 2019). A metabolite profiling study identified a direct correlation between the consumption of glycine and cell proliferation rates. Thus, authors suggested that rapidly proliferating cancer cells may preferentially take up glycine (Jain et al., 2012) and even suggested glycine metabolism as a potential target for cancer therapy (Jain et al., 2012; Maneikyte et al., 2019). Another experimental in vivo study demonstrated reduced CRC tumor growth after dietary serine and glycine was restricted (Maddocks et al., 2017). However, Labuschagne et al. was able to further clarify this relationship. The study extensively investigated glycine and serine's role in the metabolism and proliferation of cancer cells and showed that restriction of exogenous glycine or depletion of its cleavage system has no impact on cancer cell proliferation as previously thought (Labuschagne et al., 2014). Despite there is consumption of glycine by highly proliferative cells, they only switch to consuming glycine after exogenous serine has been fully depleted (Labuschagne et al., 2014). Therefore, the previous correlations between glycine uptake and cell proliferation are not causative, but rather reflect the rapid depletion of exogenous serine (Labuschagne et al., 2014). Our study did not demonstrate the pro-tumorigenic properties of glycine in vitro, as CC531 viability did not increase even if cells were exposed to very high (up to 8 mM) doses of glycine (Maneikyte et al., 2019).

Despite some existing evidence of the anti-tumorigenic potential of glycine in vitro and in vivo (Bruns et al., 2016, 2014; Rose et al., 1999b, 1999a), it has not been used in clinical trials due to the unknown interactions between glycine and conventional chemotherapy. Our study has been the first to show that glycine with 5-FU or OX does not impair their cytotoxic effectiveness in vitro. Glycine did not increase cancer cells proliferation in vivo as measured by the Ki67 tumor proliferation index (Maneikyte et al., 2019). Ki67 is among the most important cell proliferation immunocytochemical markers (Zhao et al., 2014). Expression of it depends on the cell cycle, Ki67 is produced by most cells except those in the resting (G0) phase (Kontzoglou et al., 2013; Maneikyte et al., 2019). In this study, glycine had no impact on the tumor proliferation index, while FOLFOX application reduced it (Maneikyte et al., 2019). However, it seems that glycine might have a synergistic antitumorigenic effect with FOLFOX chemotherapy by working through different pathways. 5-FU-induced cytotoxicity and cell death is mediated by its ability to disrupt nucleoside metabolism and to be incorporated into RNA/DNA (Zhang et al., 2008). Oxaliplatin, a

3rd generation diaminocyclohexane platinum compound, disrupts DNA replication by forming intrastrand links between two neighboring guanine residues or between guanine and adenine (Arango et al., 2004). While both 5-FU and OX have direct cytotoxic effects, glycine reduces tumor vascularization. Combinations of antiangiogenic agents with conventional chemotherapy are effective and used in clinical practice. One of the most widely available antiangiogenic drugs is bevacizumab, a recombinant humanized monoclonal antibody targeting the VEGF-A (Mody et al., 2018). Similar to the effects of glycine, preclinical studies demonstrated that bevacizumab reduces tumor volume, MVD, and liver metastases in murine CRC models (Mody et al., 2018). In a clinical setting, bevacizumab is effective for metastatic CRC a typically used in combination with 5-FU-based chemotherapy (Mody et al., 2018). Despite proven anti-cancer efficacy, it has some drawbacks. Bevacizumab may cause serious adverse events including neutropenia, proteinuria, hypertension, gastrointestinal perforations, hemorrhage, and wound healing complications (Mody et al., 2018). It is also related to an increased risk of various thromboembolic events (Mody et al., 2018). Therefore, it is risky in patients with some underlying medical conditions, including poorly controllable hypertension, advanced atherosclerosis, bleeding diatheses, severe proteinuria, and those who are scheduled for surgery at least 4 weeks prior and 6 weeks after treatment (Mody et al., 2018). Besides bevacizumab, 3 other antiangiogenic agents are also currently available. First, Regorafenib, an oral multikinase inhibitor that inhibits the activity of angiogenic (VEGFR-1, VEGFR-2, VEGFR-3, TIE2), stromal (PDGFR, FGFR), and oncogenic (KIT, RET, RAF-1, BRAF, BRAFV600E) kinases (Røed Skårderud et al., 2018). A recent double-blind, placebo-controlled multicenter RCT demonstrated that regorafenib combined with 5-FU-based CTx improved progression-free survival and tumor response rates (Sanoff et al., 2018). Therefore, it is currently approved as a second-line regimen for metastatic CRC patients who failed with first-line standard therapy. The second available agent is ramucirumab, a monoclonal antibody against VEGF receptor 2 (Mody et al., 2018). The phase III RAISE RCT showed that ramucirumab added to conventional 5-FU-based CTx improves the overall survival of patients who had disease progression with first-line treatment (Tabernero et al., 2015). Lastly, ziv-aflibercept, a fully-humanized monoclonal antibody that has antiangiogenic properties, has been deemed effective (Mody et al., 2018). It is a fusion protein that stops angiogenesis by binding to all isoforms of VEGF-A, VEGF-B, and

PlGF. This drug is sometimes known as a "VEGF trap" or a composite decoy receptor (Mody et al., 2018). The VELOUR RCT showed that ziv-aflibercept combined with 5-FU-based chemotherapy improved response rates as well as overall- and disease-free survival of metastatic CRC patients who progressed on previous OX-based CTx (Van Cutsem et al., 2012). Besides these three agents, there have been numerous studies that investigated plenty of other antiangiogenics - brivanib, axitinib, sunitinib, sorafenib, and cediranib. Although no promising results were seen (Mody et al., 2018). The available antiangiogenic agents, regorafenib, ramucirumab, and ziv-aflibercept, also carry the risk of various adverse events, similarly to bevacizumab. These include various skin reactions, arterial thrombosis, bleeding, neutropenia, hypertension or proteinuria (Elice and Rodeghiero, 2012; Riechelmann and Grothey, 2017). Contrary, dietary or intravenously used glycine has no such toxicities as reported by clinical trials in non-oncological settings (Evins et al., 2000; Gannon et al., 2002; Kaufman et al., 2009). Moreover, an experimental study by Mikalauskas et al. showed hepatoprotective effect of glycine against FOLFOX/FOLFIRI-induced liver injury (Mikalauskas et al., 2011). Dietary glycine significantly decreases transaminases level, microvesicular steatosis, and Kupffer cell activity after FOLFOX (Mikalauskas et al., 2011). Also it decreases leukocyte adherence in subacinar zones, prevents CTx-induced expression of inducible nitric oxide synthase, and increases microcirculation within liver (Mikalauskas et al., 2011).

Although combination regimens with antiangiogenic agents and 5-FU-based chemotherapy have proved to be effective, our study did not reveal a significant antitumorigenic effect of glycine and FOLFOX compared to that of glycine alone (Maneikyte et al., 2019). It should be considered that only one cycle of FOLFOX chemotherapy was applied in the present study, in contrast to several cycles used in routine clinical practice (Maneikyte et al., 2019). However, more cycles of FOLFOX and longer observation of experimental animals was not possible, as FOLFOX resulted in severe adverse effects (leucopenia, significant weight loss) and poor general conditions of the animals (Maneikyte et al., 2019). Delayed sacrification of study animals would have conflicted with modern laboratory animal welfare standards and laws (Maneikyte et al., 2019). However, even one cycle of FOLFOX reduced tumor cells proliferation index by Ki67 in vivo. Thus, we could speculate, that tumor growth would have been inhibited in the long term (Maneikyte et al., 2019).

The usage of 5-FU-based CTx, such as FOLFOX, may be limited because of its various side effects. These include cardiotoxicity, which usually manifests already after the 1st cycle of treatment (Maneikyte et al., 2020; Sara et al., 2018). The reported rate of 5-FU-induced cardiotoxicity varies between 1 % and 68 % and is about 8.5% in specific CRC patient cohorts (Jensen et al., 2010; Labianca et al., 1982; Maneikyte et al., 2020; Rezkalla et al., 1989; Yeh and Bickford, 2009). Furthermore, the incidence of cardiotoxic events seems to increase when fluoropyrimidines are combined with OX (Kwakman et al., 2017; Maneikyte et al., 2020; Morrow and Hoff, 2006) as it is in the FOLFOX CTx scheme and this experimental study.

5-FU-induced cardiotoxicity pathogenesis is not absolutely clear, and there is even less known about the mechanisms included in OX-induced cardiotoxicity (Depetris et al., 2018; Maneikyte et al., 2020; Oun et al., 2018). The leading hypothesis is coronary vasospasm-induced 5-FU-related myocardial ischemia (Sara et al., 2018). Clinically, 5-FU may cause myocardial ischemic symptoms followed by ECG changes seen in coronary occlusion, such as ST-segment elevation and increased levels of myocardial injury markers (i.e. troponin). However, generally, there is no evidence of macrovascular disease in angiography or CT imaging (Sara et al., 2018). The vasospasm may be related to endothelial injury-dependent or independent mechanisms (Sara et al., 2018). The latter involves primary smooth muscle dysfunction (Sara et al., 2018). Concentration-dependent vasoconstriction has been seen in rabbit aorta rings after exposure to 5-FU as well as its reversal with nitroglycerine (Mosseri et al., 1993). Also, 5-FU was shown to induce brachial artery vasoconstriction (Südhoff et al., 2004). This suggests that the main driver of 5-FU-induced cardiotoxicity is endothelium-independent vasoconstriction of vascular smooth muscle. However, there is a lack of data confirming coronary vasospasm at the time of symptoms or even after reintroducing 5-FU (Sara et al., 2018). Furthermore, pharmacologic provocation with the vasoconstrictor-alkaloid ergonovine does not induce vasospasm among patients with suspected 5-FU-induced cardiotoxicity (Sara et al., 2018). Other inconsistencies include the delayed onset of toxicity after infusion of 5-FU and the unclear role of antianginal therapy (Sara et al., 2018).

Other theories explaining 5-FU-induced cardiotoxicity include direct myocardial cell toxicity or endothelial injury resulting in a procoagulant state (Depetris et al., 2018; Jensen et al., 2010; Maneikyte et al., 2020; Mosseri et al., 1993; Porta et al., 1998). Few preclinical studies proposed mechanisms for direct cardiomyocyte injury caused by fluoropyrimidines including induction of nuclear alteration, cytoplasmic vacuolization, membrane injury, autophagy also oxidative stress-related mechanisms, and the release of free radicals, (Focaccetti et al., 2015; Lamberti et al., 2014, 2012; Maneikyte et al., 2020). All these changes cause cell death via the apoptotic pathway and result in cardiotoxicity (Maneikyte et al., 2020). Besides cardiomyocytes, fluoropyrimidines also damage endothelial cells (Cwikiel et al., 1995), which can lead to subsequent endothelial dysfunction. In addition, platinum-based agents can cause direct myocardial injury via reactive oxygen species (Maneikyte et al., 2020; Oun et al., 2018). Cardiomyocytes can overcome apoptotic injury caused by cytotoxic agents (Lamberti et al., 2012). However, these mechanisms are not effective when exposed to agents with very high oxidative potential (Lamberti et al., 2012), such as 5-FU. Experimental studies have demonstrated increased levels of reactive oxygen species and impaired activity of antioxidative systems in experimental animals treated with 5-FU (Sara et al., 2018). Such changes can disrupt cellular function by oxidizing proteins, lipids, and other macromolecules (Sara et al., 2018). Moreover, the role of reactive oxygen species in mechanisms of cardiotoxicity was further proved after N-acetyl cysteine, which is a scavenger, managed to prevent apoptosis in cardiomyocytes treated by 5-FU (Lamberti et al., 2012).

Our present study demonstrates direct cardiomyocyte toxicity by FOLFOX. The hearts of rats treated with FOLFOX presented a more than threefold higher number of apoptotic cells (Maneikyte et al., 2020). The ability of 5-FU to cause cardiomyocyte apoptosis in vitro was documented previously (Lamberti et al., 2012), but our study was the first to show it in vivo. Direct myocardial toxicity is not caused by 5-FU itself, but its metabolites α-fluoro-β-alanine (FBAL) and subsequent fluoroacetate (FAC) (Arellano et al., 1998; Guo et al., 2003; Sara et al., 2018). This has been evidenced by the use of dihydropyrimidine dehydrogenase (DPD) enzyme inhibitors to block 5-FU metabolization to FBAL and subsequently prevent cardiac injury. It has been shown to reduce the risk of repeated cardiotoxic events in patients with a history of 5-FU-induced cardiotoxicity (Sara et al., 2018). Similarly, platinum-based agents such as oxaliplatin used in our study can also cause a direct, reactive oxygen species-mediated injury to the heart.

Our study demonstrated significant myocardial fibrosis after FOLFOX application. When cardiomyocyte death occurs, healthy tissue is replaced by fibrous tissue, indicating myocardial remodeling (Salata et al., 2014). Morphologically, the major mechanisms of cardiac remodeling are cardiomyocyte apoptosis or necrosis resulting in cardiomyocyte hypertrophy and the growth of interstitial cells, especially fibroblasts (Salata et al., 2014). Physiologically these are necessary to maintain heart structure and function (Cowling et al., 2019). Cardiac fibroblasts produce many different structural and provisional proteins and the most important among them being collagen I and collagen III (Cowling et al., 2019). These extracellular matrix (ECM) proteins are key compounds that form heart fibrous meshwork (Cowling et al., 2019). Atypical quantities of ECM proteins, their quality, or abnormal proportion of individual ECM components (including alterations in the proportion of non-collagen to collagen matrix components and/or relative amounts of collagen I and collagen III) disrupts the standard structure of ECM and can lead to cardiac fibrosis (Cowling et al., 2019). Our study demonstrated that FOLFOX caused an imbalance of collagen genes expression in heart tissue by upregulating the type I collagen gene and not affecting type III collagen gene expression. Furthermore, electron microscopy analysis revealed collagen fibers in heart muscle and lysosomes in endothelial cells in the hearts of animals who received CTx and a control diet. Thus, supporting FOLFOX-induced cardiac injury. These findings show that FOLFOX has a direct cytotoxic effect on cardiomyocytes via apoptosis. Cardiac remodeling is initiated and ECM structure is disrupted with likely changes in proportions of collagen I and III, all leading to increased cardiac fibrosis.

In addition to FOLFOX-induced pathologic changes in myocardial tissue, our study also found reduced LV function in animals treated with FOLFOX chemotherapy. Repeated measurements and the decline of LVEF from baseline levels are among the most common methods to detect cardiotoxicity (Tan and Scherrer-Crosbie, 2014). The significant decline of LVEF at or after chemotherapy is associated with symptomatic heart failure (Tan and Scherrer-Crosbie, 2014). Such findings were not unexpected because myocardial fibrosis and remodeling, which were observed in our study, are the main causes of LV dysfunction. Also, it is independent predictor for different adverse cardiovascular events (Meléndez and Hundley, 2016). Previously, only anthracyclines-based chemotherapy was shown to induce cardiac fibrosis and subsequent LV dysfunction (Farhad et al., 2016). Our experimental study was the first to demonstrate similar changes after 5-FU and OX-based chemotherapy. Furthermore, the decline of LVEF after FOLFOX correlated with myocardial fibrosis and h-FABP level (Maneikyte et al., 2020). H-

FABP is a small protein that can be found in the cytosol of cardiomyocytes and is rapidly released into the systemic circulation after myocardial injury. Thus it is one of the earliest plasma markers available (ElGhandour et al., 2009) and can predict cardiovascular events in heart failure (Rezar et al., 2020). ElGhandour et al. investigated h-FABP as a biomarker for cardiotoxicity in patients undergoing treatment with 6 cycles of anthracycline-based CTx and managed to show it as an early and reliable marker (ElGhandour et al., 2009). h-FABP should appear in the systemic circulation within 90 minutes after cardiomyocytes injury and should return to physiological values within the next 36 hours (Haltern et al., 2010; Horacek et al., 2014; Maneikyte et al., 2020; Turan et al., 2017). Thus, it was unexpected that we detected significantly increased levels of this marker 7 days after FOLFOX administration (Maneikyte et al., 2020). The delayed onset of 5-FU cardiotoxicity may be explained by the previously mentioned fact, that cardiomyocytes injury is caused by 5-FU metabolites (Arellano et al., 1998; Guo et al., 2003; Maneikyte et al., 2020; Sara et al., 2018). These metabolites and their derivatives such as a-fluoro-f-hydroxypropionic acid (FHPA) are highly cardiotoxic (Arellano et al., 1998; Maneikyte et al., 2020; Meldrum et al., 1957; Reis-Mendes et al., 2015; Zhang et al., 1992). Therefore, the onset of 5-FU-based chemotherapy cardiotoxicity may be postponed until a critical level of cardiotoxic metabolites accumulates (Maneikyte et al., 2020).

The results of this study demonstrate the cardioprotective properties of glycine against FOLFOX chemotherapy-induced cardiotoxicity in CRLM treatment model in rats (Maneikyte et al., 2020). Dietary glycine not only preserved LVEF but also has been shown to reduce the levels of apoptosis and fibrosis in the hearts of experimental animals (Maneikyte et al., 2020). Furthermore, h-FABP, a myocardial injury biomarker, was markedly elevated after FOLFOX CTx irrespective of diet but was noticeably lower in animals who received glycine (Maneikyte et al., 2020). The exact pathomechanisms of how glycine prevents cardiotoxicity remain unclear, but several processes can be considered (Maneikyte et al., 2020). First, glycine decreases human and rat platelet aggregation and boosts microcirculation (Maneikyte et al., 2020; Schemmer et al., 2013; Zhong et al., 1996). Second, recently published results from a few different in vivo studies confirmed the antioxidative properties of glycine (Maneikyte et al., 2020; Ruiz-Ramírez et al., 2014; Wang et al., 2014). Since the proposed mechanisms of 5-FU-induced cardiotoxicity includes vasoconstriction, hypercoagulability caused by endothelial injury, and direct myocardial cell toxicity driven by reactive oxygen species, it looks like that glycine may counteract all of these pathophysiologic mechanisms (Depetris et al., 2018; Jensen et al., 2010; Maneikyte et al., 2020; Mosseri et al., 1993; Porta et al., 1998). The present study showed that glycine decreases FOLFOX-induced cardiac fibrosis, and these results were consistent with previous reports of anti-fibrotic properties of glycine in preclinical models of liver disease and Duchenne muscular dystrophy (Ham et al., 2019; Maneikyte et al., 2020; Rivera et al., 2001; Senthilkumar and Nalini, 2004). Since myocardial fibrosis is the main component in LV dysfunction and reduced LVEF pathogenesis, prevention by dietary glycine may have a key role in heart protection (Hinderer and Schenke-Layland, 2019; Maneikyte et al., 2020). Ultimately, these findings along with the antitumorigenic properties of glycine demonstrated in our study suggest it may be promising in oncological treatment. Glycine can improve treatment outcomes and prevent cardiotoxicity in patients who need FOLFOX for CRLM. These encouraging results warrant further study in clinical trial.

It is important to note, that there is some contrary evidence that glycine may have cardiotoxic effects (Hahn R. G., 2006; Maneikyte et al., 2020; Olsson and Hahn, 1999; Zhang et al., 1995). In vitro, 1 % and 1.5 % glycine has mild cardiotoxic properties on cardiomyocytes isolated from Sprague-Dawley rats (Zhang et al., 1995). Arrhythmias resulting in death of rabbit models were documented by Hahn et al. after infusion of 1.5 % glycine (R. Hahn et al., 1996). This solution also decreased intracellular potassium and chlorine levels in myocardial cells as demonstrated by X-ray microanalysis (R. Hahn et al., 1996). Another study investigating the impact of intravenous 1.1-2.2 % glycine in mice hearts showed potential cardiotoxic effects (R. G. Hahn et al., 1996). Half the animals treated with glycine developed extensive dilatation of the cardiac interstitium coinciding with increased myoglobin levels. Multiple infusions of glycine were associated with focal necrosis, the reaction of inflammatory cells, and myocardial tissue replacement with fibrous and granulation tissue (R. G. Hahn et al., 1996). Likewise, another experimental study showed that 1.5 % glycine infusion was associated with hypoxic lesions in the subendocardium and rupture of the histoskeleton in mice (Hahn et al., 2000). However, these cardiotoxic events occurred at glycine doses which cannot be achieved when using glycine as a dietary drug (Evins et al., 2000; Hahn R. G., 2006; Luntz et al., 2005; Maneikyte et al., 2020). Our study specifically investigated this and proved that glycine concentrations up to 8 mM, which approximately is equivalent to 0.06 % solution, did not have unfavorable effects on the growth and viability of cardiomyocytes (Maneikyte et al., 2020). Moreover, glycine already has been tested in clinical trials and none of them found relevant amino acid-induced toxicity (Evins et al., 2000; Luntz et al., 2005; Maneikyte et al., 2020). Taken together, there is evidence that glycine can be cardiotoxic only at very high concentrations. At lower concentrations as used in this study, it is not cardiotoxic but even cardioprotective against FOLFOX-induced injury (Maneikyte et al., 2020).

Our study has some limitations that should be acknowledged and considered. First, the uptake of the study drug (dietary glycine) significantly decreased after experimental animals were treated with FOLFOX chemotherapy (Maneikyte et al., 2019). Reduced dietary glycine uptake resulted in decreased plasma glycine concentration in one of the study groups. Thus, this may have prevented us from detecting the highest antitumorigenic potential of combined treatment with FOLFOX and glycine (Maneikyte et al., 2019). The second limitation was the short follow-up period in animals status-post chemotherapy. The time range may have been too short to demonstrate that FOLFOX inhibits CRLM growth (Maneikyte et al., 2019). Unfortunately, 5-FU and OX-based chemotherapy undoubtedly harmed the general condition of the study animals, and this deterioration was ongoing (Maneikyte et al., 2019). Thus, long observation of the experimental animals was not feasible as it would have conflicted with modern ethical standards (Maneikyte et al., 2019). Third, our study did not investigate the impact of FOLFOX on the microvasculature, endothelial function, and biomarkers of myocardial fibrosis (i.e. soluble suppression of tumorigenicity 2 receptor and galectin-3) that could provide more insight into the mechanisms of FOLFOX induced cardiac injury. The limited amount of biological material prevented us from a more comprehensive analysis. Fourth, the sample size of the study was relatively small and may have led to insufficient power and type 2 errors (Maneikyte et al., 2019). Despite these limitations, our study managed to show that glycine inhibits CRLM growth and tumor microvascularization (Maneikyte et al., 2020, 2019). These novel findings in tandem with previous knowledge of glycine‘s low toxicity and hepatoprotective features make it an attractive substance for oncological clinical trials.

To conclude, our study shows that glycine decreases CRLM volume likely through the reduction of MVD in tumors. Because of these anti-angiogenic properties, glycine can be used as an additive to conventional FOLFOX chemotherapy. Compared to currently used anti-angiogenic agents, glycine is not toxic. Moreover, this study demonstrated that glycine can prevent FOLFOX-induced cardiotoxicity. Clinical trials are warranted to transition these findings from bench to bedside.

5. References

Akgül, Ö., Çetinkaya, E., Ersöz, Ş., Tez, M., 2014. Role of surgery in colorectal cancer liver metastases. World J. Gastroenterol. 20, 6113–6122. https://doi.org/10.3748/wjg.v20.i20.6113

Al Bandar, M.H., Kim, N.K., 2017. Current status and future perspectives on treatment of liver metastasis in colorectal cancer (Review). Oncol. Rep. 37, 2553–2564. https://doi.org/10.3892/or.2017.5531

Al-Saeedi, M., Liang, R., Schultze, D.P., Nickkholgh, A., Herr, I., Zorn, M., Schemmer, P., 2019. Glycine protects partial liver grafts from Kupffer cell-dependent ischemia-reperfusion injury without negative effect on regeneration. Amino Acids 51, 903–911. https://doi.org/10.1007/s00726-019-02722-5

Aran, V., Victorino, A.P., Thuler, L.C., Ferreira, C.G., 2016. Colorectal Cancer: Epidemiology, Disease Mechanisms and Interventions to Reduce Onset and Mortality. Clin. Colorectal Cancer 15, 195–203. https://doi.org/10.1016/j.clcc.2016.02.008

Arango, D., Wilson, A.J., Shi, Q., Corner, G.A., Arañes, M.J., Nicholas, C., Lesser, M., Mariadason, J.M., Augenlicht, L.H., 2004. Molecular mechanisms of action and prediction of response to oxaliplatin in colorectal cancer cells. Br. J. Cancer 91, 1931–1946. https://doi.org/10.1038/sj.bjc.6602215

Arellano, M., Malet-Martino, M., Martino, R., Gires, P., 1998. The anti-cancer drug 5-fluorouracil is metabolized by the isolated perfused rat liver and in rats into highly toxic fluoroacetate. Br. J. Cancer 77, 79–86.

Argilés, G., Tabernero, J., Labianca, R., Hochhauser, D., Salazar, R., Iveson, T., Laurent-Puig, P., Quirke, P., Yoshino, T., Taieb, J., Martinelli, E., Arnold, D., ESMO Guidelines Committee. Electronic address: clinicalguidelines@esmo.org, 2020. Localised colon cancer: ESMO Clinical Practice Guidelines for diagnosis, treatment and follow-up. Ann.

Oncol. Off. J. Eur. Soc. Med. Oncol. 31, 1291–1305. https://doi.org/10.1016/j.annonc.2020.06.022

Arnold, M., Sierra, M.S., Laversanne, M., Soerjomataram, I., Jemal, A., Bray, F., 2017. Global patterns and trends in colorectal cancer incidence and mortality. Gut 66, 683–691. https://doi.org/10.1136/gutjnl-2015-310912

Ascher, E., Hanson, J.N., Cheng, W., Hingorani, A., Scheinman, M., 2001. Glycine preserves function and decreases necrosis in skeletal muscle undergoing ischemia and reperfusion injury. Surgery 129, 231–235. https://doi.org/10.1067/msy.2001.112594

Batta H. Abd El Azim, n.d. Biochemical studies of captopril against 5-Flurouracil induced heart Toxicity in rats.

Becker, R.C., 1991. Seminars in thrombosis, thrombolysis and vascular biology. 3. Platelet activity in cardiovascular disease. Cardiology 79, 49–63. https://doi.org/10.1159/000174860

Belachew, S., Malgrange, B., Rigo, J.M., Rogister, B., Leprince, P., Hans, G., Nguyen, L., Moonen, G., 2000. Glycine triggers an intracellular calcium influx in oligodendrocyte progenitor cells which is mediated by the activation of both the ionotropic glycine receptor and Na+-dependent transporters. Eur. J. Neurosci. 12, 1924–1930. https://doi.org/10.1046/j.1460-9568.2000.00085.x

Bray, F., Ferlay, J., Soerjomataram, I., Siegel, R.L., Torre, L.A., Jemal, A., 2018. Global cancer statistics 2018: GLOBOCAN estimates of incidence and mortality worldwide for 36 cancers in 185 countries. CA. Cancer J. Clin. 68, 394–424. https://doi.org/10.3322/caac.21492

Brenner, H., Kloor, M., Pox, C.P., 2014. Colorectal cancer. Lancet Lond. Engl. 383, 1490–1502. https://doi.org/10.1016/S0140-6736(13)61649-9

Bruns, H., Kazanavicius, D., Schultze, D., Saeedi, M.A., Yamanaka, K., Strupas, K., Schemmer, P., 2016. Glycine inhibits angiogenesis in colorectal cancer: role of endothelial cells. Amino Acids 48, 2549–2558. https://doi.org/10.1007/s00726-016-2278-0

Bruns, H., Petrulionis, M., Schultze, D., Al Saeedi, M., Lin, S., Yamanaka, K., Ambrazevičius, M., Strupas, K., Schemmer, P., 2014. Glycine inhibits angiogenic signaling in human hepatocellular carcinoma cells. Amino Acids 46, 969–976. https://doi.org/10.1007/s00726-013-1662-2

Byard, R.W., Harrison, R., Wells, R., Gilbert, J.D., 2001. Glycine toxicity and unexpected intra-operative death. J. Forensic Sci. 46, 1244–1246.

Cassidy, J., Clarke, S., Díaz-Rubio, E., Scheithauer, W., Figer, A., Wong, R., Koski, S., Lichinitser, M., Yang, T.-S., Rivera, F., Couture, F., Sirzén, F., Saltz, L., 2008. Randomized Phase III Study of Capecitabine Plus Oxaliplatin Compared With Fluorouracil/Folinic Acid Plus Oxaliplatin As First-Line Therapy for Metastatic Colorectal Cancer. J. Clin. Oncol. 26, 2006–2012. https://doi.org/10.1200/JCO.2007.14.9898

Ceyhan, G.O., Timm, A.-K., Bergmann, F., Günther, A., Aghdassi, A.A., Demir, I.E., Mayerle, J., Kern, M., Lerch, M.M., Büchler, M.W., Friess, H., Schemmer, P., 2011. Prophylactic glycine administration attenuates pancreatic damage and inflammation in experimental acute pancreatitis. Pancreatol. Off. J. Int. Assoc. Pancreatol. IAP Al 11, 57–67. https://doi.org/10.1159/000325972

Collins, C., Weiden, P.L., 1987. Cardiotoxicity of 5-fluorouracil. Cancer Treat. Rep. 71, 733–736.

Comprehensive molecular characterization of human colon and rectal cancer, 2012. . Nature 487, 330–337. https://doi.org/10.1038/nature11252

Cowling, R.T., Kupsky, D., Kahn, A.M., Daniels, L.B., Greenberg, B.H., 2019. Mechanisms of cardiac collagen deposition in experimental models and human disease. Transl. Res. J. Lab. Clin. Med. 209, 138. https://doi.org/10.1016/j.trsl.2019.03.004

Cutsem, E.V., Cervantes, A., Nordlinger, B., Arnold, D., 2014. Metastatic colorectal cancer: ESMO Clinical Practice Guidelines for diagnosis, treatment and follow-up †. Ann. Oncol. 25, iii1–iii9. https://doi.org/10.1093/annonc/mdu260

Cwikiel, M., Zhang, B., Eskilsson, J., Wieslander, J.B., Albertsson, M., 1995. The influence of 5-fluorouracil on the endothelium in small arteries. An electron microscopic study in rabbits. Scanning Microsc. 9, 561–576.

de Forni, M., Malet-Martino, M.C., Jaillais, P., Shubinski, R.E., Bachaud, J.M., Lemaire, L., Canal, P., Chevreau, C., Carrié, D., Soulié, P., 1992. Cardiotoxicity of high-dose continuous infusion fluorouracil: a prospective clinical study. J. Clin. Oncol. Off. J. Am. Soc. Clin. Oncol. 10, 1795–1801. https://doi.org/10.1200/JCO.1992.10.11.1795

Dekker, E., Tanis, P.J., Vleugels, J.L.A., Kasi, P.M., Wallace, M.B., 2019. Colorectal cancer. The Lancet 394, 1467–1480. https://doi.org/10.1016/S0140-6736(19)32319-0

den Butter, G., Lindell, S.L., Sumimoto, R., Schilling, M.K., Southard, J.H., Belzer, F.O., 1993. Effect of glycine in dog and rat liver transplantation. Transplantation 56, 817–822. https://doi.org/10.1097/00007890-199310000-00007

Depetris, I., Marino, D., Bonzano, A., Cagnazzo, C., Filippi, R., Aglietta, M., Leone, F., 2018. Fluoropyrimidine-induced cardiotoxicity. Crit. Rev. Oncol. Hematol. 124, 1–10. https://doi.org/10.1016/j.critrevonc.2018.02.002

Disibio, G., French, S.W., 2008. Metastatic patterns of cancers: results from a large autopsy study. Arch. Pathol. Lab. Med. 132, 931–939. https://doi.org/10.5858/2008-132-931-MPOCRF

Dolan, A.T., Diamond, S.L., 2014. Systems Modeling of Ca2+ Homeostasis and Mobilization in Platelets Mediated by IP3 and Store-Operated Ca2+ Entry. Biophys. J. 106, 2049–2060. https://doi.org/10.1016/j.bpj.2014.03.028

ElGhandour, A.H., Sorady, M.E., Azab, S., ElRahman, M., 2009. Human heart-type fatty acid-binding protein as an early diagnostic marker of doxorubicin cardiac toxicity. Hematol. Rev. 1. https://doi.org/10.4081/hr.2009.e6

Elice, F., Rodeghiero, F., 2012. Side effects of anti-angiogenic drugs. Thromb. Res. 129 Suppl 1, S50-53. https://doi.org/10.1016/S0049-3848(12)70016-6

Evins, A.E., Fitzgerald, S.M., Wine, L., Rosselli, R., Goff, D.C., 2000. Placebo-Controlled Trial of Glycine Added to Clozapine in Schizophrenia. Am. J. Psychiatry 157, 826–828. https://doi.org/10.1176/appi.ajp.157.5.826

Fang, L., Yang, Z., Zhou, J., Tung, J.-Y., Hsiao, C.-D., Wang, L., Deng, Y., Wang, P., Wang, J., Lee, M.-H., 2015. Circadian clock gene CRY2 degradation is involved in chemoresistance of colorectal cancer. Mol. Cancer Ther. 14, 1476. https://doi.org/10.1158/1535-7163.MCT-15-0030

Farhad, H., Staziaki, P.V., Addison, D., Coelho-Filho, O.R., Shah, R.V., Mitchell, R.N., Szilveszter, B., Abbasi, S.A., Kwong, R.Y., Scherrer-Crosbie, M., Hoffmann, U., Jerosch-

Herold, M., Neilan, T.G., 2016. Characterization of the Changes in Cardiac Structure and Function in Mice Treated With Anthracyclines Using serial Cardiac Magnetic Resonance Imaging. Circ. Cardiovasc. Imaging 9, e003584. https://doi.org/10.1161/CIRCIMAGING.115.003584

Focaccetti, C., Bruno, A., Magnani, E., Bartolini, D., Principi, E., Dallaglio, K., Bucci, E.O., Finzi, G., Sessa, F., Noonan, D.M., Albini, A., 2015. Effects of 5-Fluorouracil on Morphology, Cell Cycle, Proliferation, Apoptosis, Autophagy and ROS Production in Endothelial Cells and Cardiomyocytes. PLOS ONE 10, e0115686. https://doi.org/10.1371/journal.pone.0115686

Gannon, M.C., Nuttall, J.A., Nuttall, F.Q., 2002. The metabolic response to ingested glycine. Am. J. Clin. Nutr. 76, 1302–1307. https://doi.org/10.1093/ajcn/76.6.1302

Glynne-Jones, R., Wyrwicz, L., Tiret, E., Brown, G., Rödel, C., Cervantes, A., Arnold, D., 2017. Rectal cancer: ESMO Clinical Practice Guidelines for diagnosis, treatment and follow-up†. Ann. Oncol., ESMO Updated Clinical Practice Guidelines 28, iv22–iv40. https://doi.org/10.1093/annonc/mdx224

Gori, T., 2011. Viscosity, platelet activation, and hematocrit: progress in understanding their relationship with clinical and subclinical vascular disease. Clin. Hemorheol. Microcirc. 49, 37–42. https://doi.org/10.3233/CH-2011-1455

Guan, Y., Kraus, S.G., Quaney, M.J., Daniels, M.A., Mitchem, J.B., Teixeiro, E., 2020. FOLFOX Chemotherapy Ameliorates CD8 T Lymphocyte Exhaustion and Enhances Checkpoint Blockade Efficacy in Colorectal Cancer. Front. Oncol. 0. https://doi.org/10.3389/fonc.2020.00586

Guetz, G.D., Uzzan, B., Nicolas, P., Cucherat, M., Morere, J.-F., Benamouzig, R., Breau, J.-L., Perret, G.-Y., 2006. Microvessel density and VEGF expression are prognostic factors in colorectal cancer. Meta-analysis of the literature. Br. J. Cancer 94, 1823. https://doi.org/10.1038/sj.bjc.6603176

Guo, X.-D., Harold, N., Saif, M.W., Schuler, B., Szabo, E., Hamilton, J.M., Monahan, B.P., Quinn, M.G., Cliatt, J., Nguyen, D., Grollman, F., Thomas, R.R., McQuigan, E.A., Wilson, R., Takimoto, C.H., Grem, J.L., 2003. Pharmacokinetic and pharmacodynamic effects of oral eniluracil, fluorouracil and leucovorin given on a weekly schedule. Cancer Chemother. Pharmacol. 52, 79–85. https://doi.org/10.1007/s00280-003-0613-0

Haggar, F.A., Boushey, R.P., 2009. Colorectal Cancer Epidemiology: Incidence, Mortality, Survival, and Risk Factors. Clin. Colon Rectal Surg. 22, 191–197. https://doi.org/10.1055/s-0029-1242458

Hahn R. G., 2006. Glycine is toxic. Acta Anaesthesiol. Scand. 50, 261–262. https://doi.org/10.1111/j.1399-6576.2006.00927.x

Hahn, R., Nennesmo, I., Rajs, J., Sundelin, B., Wróblewski, R., Zhang, W., 1996. Morphological and X-ray microanalytical changes in mammalian tissue after overhydration with irrigating fluids. Eur. Urol. https://doi.org/10.1159/000473775

Hahn, R.G., Olsson, J., Sótonyi, P., Rajs, J., 2000. Rupture of the myocardial histoskeleton and its relation to sudden death after infusion of glycine 1.5% in the mouse. APMIS Acta Pathol. Microbiol. Immunol. Scand. 108, 487–495. https://doi.org/10.1034/j.1600-0463.2000.d01-87.x

Hahn, R.G., Zhang, W., Rajs, J., 1996. Pathology of the heart after overhydration with glycine solution in the mouse. APMIS Acta Pathol. Microbiol. Immunol. Scand. 104, 915–920. https://doi.org/10.1111/j.1699-0463.1996.tb04958.x

Hall, J.C., 1998. Glycine. JPEN J. Parenter. Enteral Nutr. 22, 393–398. https://doi.org/10.1177/0148607198022006393

Haltern, G., Peiniger, S., Bufe, A., Reiss, G., Gülker, H., Scheffold, T., 2010. Comparison of usefulness of heart-type fatty acid binding protein versus cardiac troponin T for diagnosis of acute myocardial infarction. Am. J. Cardiol. 105, 1–9. https://doi.org/10.1016/j.amjcard.2009.08.645

Ham, D.J., Gardner, A., Kennedy, T.L., Trieu, J., Naim, T., Chee, A., Alves, F.M., Caldow, M.K., Lynch, G.S., Koopman, R., 2019. Glycine administration attenuates progression of dystrophic pathology in prednisolone-treated dystrophin/utrophin null mice. Sci. Rep. 9, 12982. https://doi.org/10.1038/s41598-019-49140-x

Hess, K.R., Varadhachary, G.R., Taylor, S.H., Wei, W., Raber, M.N., Lenzi, R., Abbruzzese, J.L., 2006. Metastatic patterns in adenocarcinoma. Cancer 106, 1624–1633. https://doi.org/10.1002/cncr.21778

Hillen, F., Griffioen, A.W., 2007. Tumour vascularization: sprouting angiogenesis and beyond. Cancer Metastasis Rev. 26, 489–502. https://doi.org/10.1007/s10555-007-9094-7

Hinderer, S., Schenke-Layland, K., 2019. Cardiac fibrosis – A short review of causes and therapeutic strategies. Adv. Drug Deliv. Rev., Wound healing and fibrosis – State of play 146, 77–82. https://doi.org/10.1016/j.addr.2019.05.011

Horacek, J.M., Vasatova, M., Pudil, R., Tichy, M., Zak, P., Jakl, M., Jebavy, L., Maly, J., 2014. Biomarkers for the early detection of anthracycline-induced cardiotoxicity: current status. Biomed. Pap. Med. Fac. Univ. Palacky Olomouc Czechoslov. 158, 511–517. https://doi.org/10.5507/bp.2014.004

Hugen, N., Velde, C.J.H. van de, Wilt, J.H.W. de, Nagtegaal, I.D., 2014. Metastatic pattern in colorectal cancer is strongly influenced by histological subtype. Ann. Oncol. 25, 651–657. https://doi.org/10.1093/annonc/mdt591

Ikejima, K., Qu, W., Stachlewitz, R.F., Thurman, R.G., 1997. Kupffer cells contain a glycine-gated chloride channel. Am. J. Physiol. 272, G1581-1586. https://doi.org/10.1152/ajpgi.1997.272.6.G1581

Jain, M., Nilsson, R., Sharma, S., Madhusudhan, N., Kitami, T., Souza, A.L., Kafri, R., Kirschner, M.W., Clish, C.B., Mootha, V.K., 2012. Metabolite Profiling Identifies a Key Role for Glycine in Rapid Cancer Cell Proliferation. Science 336, 1040–1044. https://doi.org/10.1126/science.1218595

Jensen, S.A., Hasbak, P., Mortensen, J., Sørensen, J.B., 2010. Fluorouracil induces myocardial ischemia with increases of plasma brain natriuretic peptide and lactic acid but without dysfunction of left ventricle. J. Clin. Oncol. Off. J. Am. Soc. Clin. Oncol. 28, 5280–5286. https://doi.org/10.1200/JCO.2009.27.3953

Kaufman, M.J., Prescot, A.P., Ongur, D., Evins, A.E., Barros, T.L., Medeiros, C.L., Covell, J., Wang, L., Fava, M., Renshaw, P.F., 2009. Oral glycine administration increases brain glycine/creatine ratios in men: a proton magnetic resonance spectroscopy study. Psychiatry Res. 173, 143–149. https://doi.org/10.1016/j.pscychresns.2009.03.004

Kontzoglou, K., Palla, V., Karaolanis, G., Karaiskos, I., Alexiou, I., Pateras, I., Konstantoudakis, K., Stamatakos, M., 2013. Correlation between Ki67 and Breast Cancer Prognosis. Oncology 84, 219–225. https://doi.org/10.1159/000346475

Kow, A.W.C., 2019. Hepatic metastasis from colorectal cancer. J. Gastrointest. Oncol. 10, 1274–1298. https://doi.org/10.21037/jgo.2019.08.06

Kwakman, J.J.M., Simkens, L.H.J., Mol, L., Kok, W.E.M., Koopman, M., Punt, C.J.A., 2017. Incidence of capecitabine-related cardiotoxicity in different treatment schedules of metastatic colorectal cancer: A retrospective analysis of the CAIRO studies of the Dutch Colorectal Cancer Group. Eur. J. Cancer Oxf. Engl. 1990 76, 93–99. https://doi.org/10.1016/j.ejca.2017.02.009

Labianca, R., Beretta, G., Clerici, M., Fraschini, P., Luporini, G., 1982. Cardiac toxicity of 5-fluorouracil: a study on 1083 patients. Tumori 68, 505–510.

Labuschagne, C.F., van den Broek, N.J.F., Mackay, G.M., Vousden, K.H., Maddocks, O.D.K., 2014. Serine, but not glycine, supports one-carbon metabolism and proliferation of cancer cells. Cell Rep. 7, 1248–1258. https://doi.org/10.1016/j.celrep.2014.04.045

Lamberti, M., Porto, S., Marra, M., Zappavigna, S., Grimaldi, A., Feola, D., Pesce, D., Naviglio, S., Spina, A., Sannolo, N., Caraglia, M., 2012. 5-Fluorouracil induces apoptosis in rat cardiocytes through intracellular oxidative stress. J. Exp. Clin. Cancer Res. 31, 60. https://doi.org/10.1186/1756-9966-31-60

Lamberti, M., Porto, S., Zappavigna, S., Addeo, E., Marra, M., Miraglia, N., Sannolo, N., Vanacore, D., Stiuso, P., Caraglia, M., 2014. A mechanistic study on the cardiotoxicity of 5-fluorouracil in vitro and clinical and occupational perspectives. Toxicol. Lett. 227, 151–156. https://doi.org/10.1016/j.toxlet.2014.03.018

Layoun, M.E., Wickramasinghe, C.D., Peralta, M.V., Yang, E.H., 2016. Fluoropyrimidine-Induced Cardiotoxicity: Manifestations, Mechanisms, and Management. Curr. Oncol. Rep. 18, 35. https://doi.org/10.1007/s11912-016-0521-1

Lazaris, A., Amri, A., Petrillo, S.K., Zoroquiain, P., Ibrahim, N., Salman, A., Gao, Z., Vermeulen, P.B., Metrakos, P., 2018. Vascularization of colorectal carcinoma liver metastasis: insight into stratification of patients for anti-angiogenic therapies. J. Pathol. Clin. Res. 4, 184–192. https://doi.org/10.1002/cjp2.100

Lee, M.A., McCauley, R.D., Kong, S.-E., Hall, J.C., 2002. Influence of glycine on intestinal ischemia-reperfusion injury. JPEN J. Parenter. Enteral Nutr. 26, 130–135. https://doi.org/10.1177/0148607102026002130

Lugano, R., Ramachandran, M., Dimberg, A., 2020. Tumor angiogenesis: causes, consequences, challenges and opportunities. Cell. Mol. Life Sci. 77, 1745–1770. https://doi.org/10.1007/s00018-019-03351-7

Luntz, S.P., Unnebrink, K., Seibert-Grafe, M., Bunzendahl, H., Kraus, T.W., Büchler, M.W., Klar, E., Schemmer, P., 2005. HEGPOL: randomized, placebo controlled, multicenter, double-blind clinical trial to investigate hepatoprotective effects of glycine in the postoperative phase of liver transplantation [ISRCTN69350312]. BMC Surg. 5, 18. https://doi.org/10.1186/1471-2482-5-18

Ma, X., Wu, Y., Zhang, T., Song, H., Jv, H., Guo, W., Ren, G., 2017. Ki67 Proliferation Index as a Histopathological Predictive and Prognostic Parameter of Oral Mucosal Melanoma in Patients without Distant Metastases. J. Cancer 8, 3828–3837. https://doi.org/10.7150/jca.20935

Maddocks, O.D.K., Athineos, D., Cheung, E.C., Lee, P., Zhang, T., Broek, N.J.F. van den, Mackay, G.M., Labuschagne, C.F., Gay, D., Kruiswijk, F., Blagih, J., Vincent, D.F., Campbell, K.J., Ceteci, F., Sansom, O.J., Blyth, K., Vousden, K.H., 2017. Modulating the therapeutic response of tumours to dietary serine and glycine starvation. Nature 544, 372. https://doi.org/10.1038/nature22056

Madeddu, C., Deidda, M., Piras, A., Cadeddu, C., Demurtas, L., Puzzoni, M., Piscopo, G., Scartozzi, M., Mercuro, G., 2016. Pathophysiology of cardiotoxicity induced by nonanthracycline chemotherapy. J. Cardiovasc. Med. Hagerstown Md 17 Suppl 1, S12-18. https://doi.org/10.2459/JCM.0000000000000376

Maeda, K., Hazama, S., Tokuno, K., Kan, S., Maeda, Y., Watanabe, Y., Kamei, R., Shindo, Y., Maeda, N., Yoshimura, K., Yoshino, S., Oka, M., 2011. Impact of Chemotherapy for Colorectal Cancer on Regulatory T-Cells and Tumor Immunity. Anticancer Res. 31, 4569–4574.

Maneikyte, J., Bausys, A., Leber, B., Feldbacher, N., Hoefler, G., Kolb-Lenz, D., Strupas, K., Stiegler, P., Schemmer, P., 2020. Dietary Glycine Prevents FOLFOX Chemotherapy-Induced Heart Injury: A Colorectal Cancer Liver Metastasis Treatment Model in Rats. Nutrients 12. https://doi.org/10.3390/nu12092634

Maneikyte, J., Bausys, A., Leber, B., Horvath, A., Feldbacher, N., Hoefler, G., Strupas, K., Stiegler, P., Schemmer, P., 2019. Dietary glycine decreases both tumor volume and vascularization in a combined colorectal liver metastasis and chemotherapy model. Int. J. Biol. Sci. 15, 1582–1590. https://doi.org/10.7150/ijbs.35513

Manne, U., Shanmugam, C., Katkoori, V.R., Bumpers, H.L., Grizzle, W.E., 2010. Development and progression of colorectal neoplasia. Cancer Biomark. Sect. Dis. Markers 9, 235–265. https://doi.org/10.3233/CBM-2011-0160

Marsh, D.C., Vreugdenhil, P.K., Mack, V.E., Belzer, F.O., Southard, J.H., 1993. Glycine Protects Hepatocytes from Injury Caused by Anoxia, Cold Ischemia and Mitochondrial Inhibitors, But Not Injury Caused by Calcium Ionophores or Oxidative Stress. Hepatology 17, 91–98. https://doi.org/10.1002/hep.1840170117

Medema, J.P., 2013. Cancer stem cells: The challenges ahead. Nat. Cell Biol. 15, 338–344. https://doi.org/10.1038/ncb2717

Meldrum, G.K., Bignell, J.T., Rowley, I., 1957. The Use of Sodium Fluoroacetate (compound 1080) for the Control of the Rabbit in Tasmania. Aust. Vet. J. 33, 186–196. https://doi.org/10.1111/j.1751-0813.1957.tb05738.x

Meléndez, G.C., Hundley, W.G., 2016. Is Myocardial Fibrosis a New Frontier for Discovery in Cardiotoxicity Related to the Administration of Anthracyclines? Circ. Cardiovasc. Imaging 9, e005797. https://doi.org/10.1161/CIRCIMAGING.116.005797

Mikalauskas, S., Mikalauskiene, L., Bruns, H., Nickkholgh, A., Hoffmann, K., Longerich, T., Strupas, K., Büchler, M.W., Schemmer, P., 2011. Dietary glycine protects from chemotherapy-induced hepatotoxicity. Amino Acids 40, 1139–1150. https://doi.org/10.1007/s00726-010-0737-6

Minotti, G., 2013. Pharmacology at Work for Cardio-Oncology: Ranolazine to Treat Early Cardiotoxicity Induced by Antitumor Drugs. J. Pharmacol. Exp. Ther. 346, 343–349. https://doi.org/10.1124/jpet.113.204057

Mody, K., Baldeo, C., Bekaii-Saab, T., 2018. Antiangiogenic Therapy in Colorectal Cancer. Cancer J. Sudbury Mass 24, 165–170. https://doi.org/10.1097/PPO.0000000000000328

Morrow, P.K., Hoff, P.M., 2006. Does the addition of oxaliplatin increase the risk of capecitabine-induced cardiotoxicity? Nat. Rev. Clin. Oncol. 3, 76–77. https://doi.org/10.1038/ncponc0398

Mosseri, M., Fingert, H.J., Varticovski, L., Chokshi, S., Isner, J.M., 1993. In vitro evidence that myocardial ischemia resulting from 5-fluorouracil chemotherapy is due to protein kinase C-mediated vasoconstriction of vascular smooth muscle. Cancer Res. 53, 3028–3033.

Munker, S., Gerken, M., Fest, P., Ott, C., Schnoy, E., Fichtner-Feigl, S., Wiggermann, P., Vogelhuber, M., Herr, W., Stroszczynski, C., Schlitt, H.J., Evert, M., Reng, M., Klinkhammer-Schalke, M., Teufel, A., 2018. Chemotherapy for metastatic colon cancer: No effect on survival when the dose is reduced due to side effects. BMC Cancer 18. https://doi.org/10.1186/s12885-018-4380-z

Nagy, J.A., Brown, L.F., Senger, D.R., Lanir, N., Van De Water, L., Dvorak, A.M., Dvorak, H.F., 1989. Pathogenesis of tumor stroma generation: a critical role for leaky blood vessels and fibrin deposition. Biochim. Biophys. Acta BBA - Rev. Cancer 948, 305–326. https://doi.org/10.1016/0304-419X(89)90004-8

Nassar, D., Blanpain, C., 2016. Cancer Stem Cells: Basic Concepts and Therapeutic Implications. Annu. Rev. Pathol. Mech. Dis. 11, 47–76. https://doi.org/10.1146/annurev-pathol-012615-044438

Nguyen, L.H., Goel, A., Chung, D.C., 2020. Pathways of Colorectal Carcinogenesis. Gastroenterology 158, 291–302. https://doi.org/10.1053/j.gastro.2019.08.059

Oleksowicz, L., Bruckner, H.W., 1988. Prophylaxis of 5-fluorouracil-induced coronary vasospasm with calcium channel blockers. Am. J. Med. 85, 750–751. https://doi.org/10.1016/s0002-9343(88)80268-7

Olsson, J., Hahn, R.G., 1999. Glycine toxicity after high-dose i.v. infusion of 1.5% glycine in the mouse. Br. J. Anaesth. 82, 250–254.

Oun, R., Moussa, Y.E., Wheate, N.J., 2018. The side effects of platinum-based chemotherapy drugs: a review for chemists. Dalton Trans. Camb. Engl. 2003 47, 6645–6653. https://doi.org/10.1039/c8dt00838h

Oun, R., Rowan, E., 2017. Cisplatin induced arrhythmia; electrolyte imbalance or disturbance of the SA node? Eur. J. Pharmacol. 811, 125–128. https://doi.org/10.1016/j.ejphar.2017.05.063

Polk, A., Vaage-Nilsen, M., Vistisen, K., Nielsen, D.L., 2013. Cardiotoxicity in cancer patients treated with 5-fluorouracil or capecitabine: a systematic review of incidence, manifestations and predisposing factors. Cancer Treat. Rev. 39, 974–984. https://doi.org/10.1016/j.ctrv.2013.03.005

Porta, C., Moroni, M., Ferrari, S., Nastasi, G., 1998. Endothelin-1 and 5-fluorouracil-induced cardiotoxicity. Neoplasma 45, 81–82.

Qian, T., Nieminen, A.L., Herman, B., Lemasters, J.J., 1997. Mitochondrial permeability transition in pH-dependent reperfusion injury to rat hepatocytes. Am. J. Physiol. 273, C1783-1792. https://doi.org/10.1152/ajpcell.1997.273.6.C1783

Rawla, P., Sunkara, T., Barsouk, A., 2019. Epidemiology of colorectal cancer: incidence, mortality, survival, and risk factors. Przegląd Gastroenterol. 14, 89–103. https://doi.org/10.5114/pg.2018.81072

Reis-Mendes, A.F., Sousa, E., de Lourdes Bastos, M., Costa, V.M., 2015. The Role of the Metabolism of Anticancer Drugs in Their Induced-Cardiotoxicity. Curr. Drug Metab. 17, 75–90.

Rezar, R., Jirak, P., Gschwandtner, M., Derler, R., Felder, T.K., Haslinger, M., Kopp, K., Seelmaier, C., Granitz, C., Hoppe, U.C., Lichtenauer, M., 2020. Heart-Type Fatty Acid-Binding Protein (H-FABP) and Its Role as a Biomarker in Heart Failure: What Do We Know So Far? J. Clin. Med. 9, 164. https://doi.org/10.3390/jcm9010164

Rezkalla, S., Kloner, R.A., Ensley, J., al-Sarraf, M., Revels, S., Olivenstein, A., Bhasin, S., Kerpel-Fronious, S., Turi, Z.G., 1989. Continuous ambulatory ECG monitoring during fluorouracil therapy: a prospective study. J. Clin. Oncol. Off. J. Am. Soc. Clin. Oncol. 7, 509–514. https://doi.org/10.1200/JCO.1989.7.4.509

Richert, M.M., Vaidya, K.S., Mills, C.N., Wong, D., Korz, W., Hurst, D.R., Welch, D.R., 2009. Inhibition of CXCR4 by CTCE-9908 inhibits breast cancer metastasis to lung and bone. Oncol. Rep. 21, 761–767.

Riechelmann, R., Grothey, A., 2017. Antiangiogenic therapy for refractory colorectal cancer: current options and future strategies. Ther. Adv. Med. Oncol. 9, 106–126. https://doi.org/10.1177/1758834016676703

Ríha, H., Papoušek, F., Neckář, J., Pirk, J., Ošťádal, B., 2012. Effects of isoflurane concentration on basic echocardiographic parameters of the left ventricle in rats. Physiol. Res. 61, 419–423.

Riihimäki, M., Hemminki, A., Sundquist, J., Hemminki, K., 2016. Patterns of metastasis in colon and rectal cancer. Sci. Rep. 6, 29765. https://doi.org/10.1038/srep29765

Rivera, C.A., Bradford, B.U., Hunt, K.J., Adachi, Y., Schrum, L.W., Koop, D.R., Burchardt, E.-R., Rippe, R.A., Thurman, R.G., 2001. Attenuation of CCl4-induced hepatic fibrosis by GdCl3 treatment or dietary glycine. Am. J. Physiol.-Gastrointest. Liver Physiol. 281, G200–G207. https://doi.org/10.1152/ajpgi.2001.281.1.G200

Røed Skårderud, M., Polk, A., Kjeldgaard Vistisen, K., Larsen, F.O., Nielsen, D.L., 2018. Efficacy and safety of regorafenib in the treatment of metastatic colorectal cancer: A systematic review. Cancer Treat. Rev. 62, 61–73. https://doi.org/10.1016/j.ctrv.2017.10.011

Rose, M.L., Cattley, R.C., Dunn, C., Wong, V., Li, X., Thurman, R.G., 1999a. Dietary glycine prevents the development of liver tumors caused by the peroxisome proliferator WY-14,643. Carcinogenesis 20, 2075–2081.

Rose, M.L., Madren, J., Bunzendahl, H., Thurman, R.G., 1999b. Dietary glycine inhibits the growth of B16 melanoma tumors in mice. Carcinogenesis 20, 793–798.

Ruggeri, Z.M., 1997. Mechanisms initiating platelet thrombus formation. Thromb. Haemost. 78, 611–616.

Ruiz-Ramírez, A., Ortiz-Balderas, E., Cardozo-Saldaña, G., Diaz-Diaz, E., El-Hafidi, M., 2014. Glycine restores glutathione and protects against oxidative stress in vascular tissue from sucrose-fed rats. Clin. Sci. 126, 19–29. https://doi.org/10.1042/CS20130164

Salata, C., Ferreira-Machado, S.C., Andrade, C.B.V.D., Mencalha, A.L., Mandarim-de-Lacerda, C.A., Almeida, C.E.V. de, 2014. Apoptosis induction of cardiomyocytes and subsequent fibrosis after irradiation and neoadjuvant chemotherapy. Int. J. Radiat. Biol. 90, 284–290. https://doi.org/10.3109/09553002.2014.887869

Sanoff, H.K., Goldberg, R.M., Ivanova, A., O'Reilly, S., Kasbari, S.S., Kim, R.D., McDermott, R., Moore, D.T., Zamboni, W., Grogan, W., Cohn, A.L., Bekaii-Saab, T.S., Leonard, G., Ryan, T., Olowokure, O.O., Fernando, N.H., McCaffrey, J., El-Rayes, B.F., Horgan, A.M., Sherrill, G.B., Yacoub, G.H., O'Neil, B.H., 2018. Multicenter, randomized, double-blind phase 2 trial of FOLFIRI with regorafenib or placebo as second-line therapy for metastatic colorectal cancer. Cancer 124, 3118–3126. https://doi.org/10.1002/cncr.31552

Sanoff, H.K., Sargent, D.J., Campbell, M.E., Morton, R.F., Fuchs, C.S., Ramanathan, R.K., Williamson, S.K., Findlay, B.P., Pitot, H.C., Goldberg, R.M., 2008. Five-Year Data and Prognostic Factor Analysis of Oxaliplatin and Irinotecan Combinations for Advanced Colorectal Cancer: N9741. J. Clin. Oncol. 26, 5721–5727. https://doi.org/10.1200/JCO.2008.17.7147

Sara, J.D., Kaur, J., Khodadadi, R., Rehman, M., Lobo, R., Chakrabarti, S., Herrmann, J., Lerman, A., Grothey, A., 2018. 5-fluorouracil and cardiotoxicity: a review. Ther. Adv. Med. Oncol. 10. https://doi.org/10.1177/1758835918780140

Schemmer, P., Bradford, B.U., Rose, M.L., Bunzendahl, H., Raleigh, J.A., Lemasters, J.J., Thurman, R.G., 1999a. Intravenous glycine improves survival in rat liver transplantation. Am. J. Physiol. 276, G924-932.

Schemmer, P., Connor, H.D., Arteel, G.E., Raleigh, J.A., Bunzendahl, H., Mason, R.P., Thurman, R.G., 1999b. Reperfusion injury in livers due to gentle in situ organ manipulation during harvest involves hypoxia and free radicals. J. Pharmacol. Exp. Ther. 290, 235–240.

Schemmer, P., Schoonhoven, R., Swenberg, J.A., Bunzendahl, H., Thurman, R.G., 1998. Gentle in situ liver manipulation during organ harvest decreases survival after rat liver transplantation: role of Kupffer cells. Transplantation 65, 1015–1020. https://doi.org/10.1097/00007890-199804270-00001

Schemmer, P., Zhong, Z., Galli, U., Wheeler, M.D., Xiangli, L., Bradford, B.U., Conzelmann, L.O., Forman, D., Boyer, J., Thurman, R.G., 2013. Glycine reduces platelet aggregation. Amino Acids 44, 925–931. https://doi.org/10.1007/s00726-012-1422-8

Schöber, C., Papageorgiou, E., Harstrick, A., Bokemeyer, C., Mügge, A., Stahl, M., Wilke, H., Poliwoda, H., Hiddemann, W., Köhne-Wömpner, C.H., 1993. Cardiotoxicity of 5-

fluorouracil in combination with folinic acid in patients with gastrointestinal cancer. Cancer 72, 2242–2247. https://doi.org/10.1002/1097-0142(19931001)72:7<2242::aid-cncr2820720730>3.0.co;2-e

Senthilkumar, R., Nalini, N., 2004. Glycine prevents hepatic fibrosis by preventing the accumulation of collagen in rats with alcoholic liver injury. Pol. J. Pharmacol. 56, 121–128.

Simon, K., 2016. Colorectal cancer development and advances in screening. Clin. Interv. Aging 11, 967–976. https://doi.org/10.2147/CIA.S109285

Sperling, J., Brandhorst, D., Schäfer, T., Ziemann, C., Benz-Weißer, A., Scheuer, C., Kollmar, O., Schilling, M.K., Menger, M.D., 2013. Liver-directed chemotherapy of cetuximab and bevacizumab in combination with oxaliplatin is more effective to inhibit tumor growth of CC531 colorectal rat liver metastases than systemic chemotherapy. Clin. Exp. Metastasis 30, 447–455. https://doi.org/10.1007/s10585-012-9550-9

Stiegler, P., Sereinigg, M., Puntschart, A., Bradatsch, A., Seifert-Held, T., Wiederstein-Grasser, I., Leber, B., Stadelmeyer, E., Dandachi, N., Zelzer, S., Iberer, F., Stadlbauer, V., 2013. Oxidative stress and apoptosis in a pig model of brain death (BD) and living donation (LD). J. Transl. Med. 11, 244. https://doi.org/10.1186/1479-5876-11-244

Südhoff, T., Enderle, M.-D., Pahlke, M., Petz, C., Teschendorf, C., Graeven, U., Schmiegel, W., 2004. 5-Fluorouracil induces arterial vasocontractions. Ann. Oncol. Off. J. Eur. Soc. Med. Oncol. 15, 661–664. https://doi.org/10.1093/annonc/mdh150

Sung, H., Ferlay, J., Siegel, R.L., Laversanne, M., Soerjomataram, I., Jemal, A., Bray, F., 2021. Global Cancer Statistics 2020: GLOBOCAN Estimates of Incidence and Mortality Worldwide for 36 Cancers in 185 Countries. CA. Cancer J. Clin. 71, 209–249. https://doi.org/10.3322/caac.21660

Tabernero, J., Yoshino, T., Cohn, A.L., Obermannova, R., Bodoky, G., Garcia-Carbonero, R., Ciuleanu, T.-E., Portnoy, D.C., Cutsem, E.V., Grothey, A., Prausová, J., Garcia-Alfonso, P., Yamazaki, K., Clingan, P.R., Lonardi, S., Kim, T.W., Simms, L., Chang, S.-C., Nasroulah, F., 2015. Ramucirumab versus placebo in combination with second-line FOLFIRI in patients with metastatic colorectal carcinoma that progressed during or after first-line therapy with bevacizumab, oxaliplatin, and a fluoropyrimidine (RAISE): a randomised, double-blind, multicentre, phase 3 study. Lancet Oncol. 16, 499–508. https://doi.org/10.1016/S1470-2045(15)70127-0

Takahashi, Y., Ellis, L.M., Mai, M., 2003. The angiogenic switch of human colon cancer occurs simultaneous to initiation of invasion. Oncol. Rep. 10, 9–13.

Tan, T.C., Scherrer-Crosbie, M., 2014. CARDIAC COMPLICATIONS OF CHEMOTHERAPY: ROLE OF IMAGING. Curr. Treat. Options Cardiovasc. Med. 16, 296. https://doi.org/10.1007/s11936-014-0296-3

Toden, S., Okugawa, Y., Jascur, T., Wodarz, D., Komarova, N.L., Buhrmann, C., Shakibaei, M., Boland, C.R., Goel, A., 2015. Curcumin mediates chemosensitization to 5-fluorouracil through miRNA-induced suppression of epithelial-to-mesenchymal transition in chemoresistant colorectal cancer. Carcinogenesis 36, 355. https://doi.org/10.1093/carcin/bgv006

Torre, L.A., Bray, F., Siegel, R.L., Ferlay, J., Lortet-Tieulent, J., Jemal, A., 2015. Global cancer statistics, 2012. CA. Cancer J. Clin. 65, 87–108. https://doi.org/10.3322/caac.21262

Turan, T., Agac, M.T., Aykan, A.Ç., Kul, S., Akyüz, A.R., Gökdeniz, T., Gül, İ., Cengiz, E., Boyacı, F., Erkan, H., Akdemir, R., Celik, S., 2017. Usefulness of Heart-Type Fatty Acid-Binding Protein and Myocardial Performance Index for Early Detection of 5-Fluorouracil Cardiotoxicity. Angiology 68, 52–58. https://doi.org/10.1177/0003319716637516

Van Cutsem, E., Tabernero, J., Lakomy, R., Prenen, H., Prausová, J., Macarulla, T., Ruff, P., van Hazel, G.A., Moiseyenko, V., Ferry, D., McKendrick, J., Polikoff, J., Tellier, A., Castan, R., Allegra, C., 2012. Addition of aflibercept to fluorouracil, leucovorin, and irinotecan improves survival in a phase III randomized trial in patients with metastatic colorectal cancer previously treated with an oxaliplatin-based regimen. J. Clin. Oncol. Off. J. Am. Soc. Clin. Oncol. 30, 3499–3506. https://doi.org/10.1200/JCO.2012.42.8201

Varga-Szabo, D., Braun, A., Nieswandt, B., 2009. Calcium signaling in platelets. J. Thromb. Haemost. 7, 1057–1066. https://doi.org/10.1111/j.1538-7836.2009.03455.x

Vatandoust, S., Price, T.J., Karapetis, C.S., 2015. Colorectal cancer: Metastases to a single organ. World J. Gastroenterol. 21, 11767–11776. https://doi.org/10.3748/wjg.v21.i41.11767

Venkatachalam, M.A., Weinberg, J.M., Patel, Y., Saikumar, P., Dong, Z., 1996. Cytoprotection of kidney epithelial cells by compounds that target amino acid gated chloride channels. Kidney Int. 49, 449–460. https://doi.org/10.1038/ki.1996.64

Vogel, A., Hofheinz, R.D., Kubicka, S., Arnold, D., 2017. Treatment decisions in metastatic colorectal cancer – Beyond first and second line combination therapies. Cancer Treat. Rev. 59, 54–60. https://doi.org/10.1016/j.ctrv.2017.04.007

Wang, W., Wu, Z., Dai, Z., Yang, Y., Wang, J., Wu, G., 2013. Glycine metabolism in animals and humans: implications for nutrition and health. Amino Acids 45, 463–477. https://doi.org/10.1007/s00726-013-1493-1

Wang, W., Wu, Z., Lin, G., Hu, S., Wang, B., Dai, Z., Wu, G., 2014. Glycine stimulates protein synthesis and inhibits oxidative stress in pig small intestinal epithelial cells. J. Nutr. 144, 1540–1548. https://doi.org/10.3945/jn.114.194001

Weiss, L., Grundmann, E., Torhorst, J., Hartveit, F., Moberg, I., Eder, M., Fenoglio-Preiser, C.M., Napier, J., Horne, C.H., Lopez, M.J., 1986. Haematogenous metastatic patterns in colonic carcinoma: an analysis of 1541 necropsies. J. Pathol. 150, 195–203. https://doi.org/10.1002/path.1711500308

Wheeler, M.D., Ikejema, K., Enomoto, N., Stacklewitz, R.F., Seabra, V., Zhong, Z., Yin, M., Schemmer, P., Rose, M.L., Rusyn, I., Bradford, B., Thurman, R.G., 1999. Glycine: a new anti-inflammatory immunonutrient. Cell. Mol. Life Sci. CMLS 56, 843–856. https://doi.org/10.1007/s000180050030

Wheeler, M.D., Rose, M.L., Yamashima, S., Enomoto, N., Seabra, V., Madren, J., Thurman, R.G., 2000. Dietary glycine blunts lung inflammatory cell influx following acute endotoxin. Am. J. Physiol. Lung Cell. Mol. Physiol. 279, L390-398. https://doi.org/10.1152/ajplung.2000.279.2.L390

Wu, G., 2010. Functional amino acids in growth, reproduction, and health. Adv. Nutr. Bethesda Md 1, 31–37. https://doi.org/10.3945/an.110.1008

Yeh, E.T.H., Bickford, C.L., 2009. Cardiovascular complications of cancer therapy: incidence, pathogenesis, diagnosis, and management. J. Am. Coll. Cardiol. 53, 2231–2247. https://doi.org/10.1016/j.jacc.2009.02.050

Zervoudakis, A., Boucher, T., Kemeny, N.E., 2017. Treatment Options in Colorectal Liver Metastases: Hepatic Arterial Infusion. Visc. Med. 33, 47–53. https://doi.org/10.1159/000454693

Zhang, N., Yin, Y., Xu, S.-J., Chen, W.-S., 2008. 5-Fluorouracil: Mechanisms of Resistance and Reversal Strategies. Molecules 13, 1551–1569. https://doi.org/10.3390/molecules13081551

Zhang, R.W., Soong, S.J., Liu, T.P., Barnes, S., Diasio, S.B., 1992. Pharmacokinetics and tissue distribution of 2-fluoro-beta-alanine in rats. Potential relevance to toxicity pattern of 5-fluorouracil. Drug Metab. Dispos. Biol. Fate Chem. 20, 113–119.

Zhang, W., Andersson, B.S., Hahn, R.G., 1995. Effect of irrigating fluids and prostate tissue extracts on isolated cardiomyocytes. Urology 46, 821–824. https://doi.org/10.1016/S0090-4295(99)80351-3

Zhao, W.-Y., Xu, J., Wang, M., Zhang, Z.-Z., Tu, L., Wang, C.-J., Lin, T.-L., Shen, Y.-Y., Liu, Q., Cao, H., 2014. Prognostic value of Ki67 index in gastrointestinal stromal tumors. Int. J. Clin. Exp. Pathol. 7, 2298–2304.

Zhong, Z., Connor, H.D., Yin, M., Moss, N., Mason, R.P., Bunzendahl, H., Forman, D.T., Thurman, R.G., 1999. Dietary glycine and renal denervation prevents cyclosporin A-induced hydroxyl radical production in rat kidney. Mol. Pharmacol. 56, 455–463. https://doi.org/10.1124/mol.56.3.455

Zhong, Z., Jones, S., Thurman, R.G., 1996. Glycine minimizes reperfusion injury in a low-flow, reflow liver perfusion model in the rat. Am. J. Physiol. 270, G332-338. https://doi.org/10.1152/ajpgi.1996.270.2.G332

Zhong, Z., Li, X., Yamashina, S., von Frankenberg, M., Enomoto, N., Ikejima, K., Kolinsky, M., Raleigh, J.A., Thurman, R.G., 2001. Cyclosporin A causes a hypermetabolic state and hypoxia in the liver: prevention by dietary glycine. J. Pharmacol. Exp. Ther. 299, 858–865.

Zhong, Z., Wheeler, M.D., Li, X., Froh, M., Schemmer, P., Yin, M., Bunzendaul, H., Bradford, B., Lemasters, J.J., 2003. L-glycine: a novel antiinflammatory, immunomodulatory, and cytoprotective agent. Curr. Opin. Clin. Nutr. Metab. Care 6, 229–240.